“SAPIENZA” UNIVERSITY OF ROME
Department of Experimental Medicine

Ph.D. program
“HUMAN BIOLOGY AND MEDICAL GENETICS”
XXXII cycle

Study of the molecular machinery controlling miRNA sorting in exosomes: a role for PCBP2

Candidate:
Giovanna Sabarese

Scientific tutor:
Prof.ssa Carla Cicchini “Sapienza” University of Rome
Dept. of Molecular Medicine

Director of Doctoral Program:
Prof. Antonio Pizzuti “Sapienza” University of Rome
Dept. of Experimental Medicine

Board of examiners:

Prof. Marco Barchi
Prof.ssa Alice Conigliaro
Prof.ssa Silvia Galardi
Prof.ssa Ornella Parolini
Prof.ssa Maria Piane

Academic year 2018-2019

INDEX

ABSTRACT

Exosomes are small, cell-secreted vesicles that carry specific repertoires of proteins and RNAs to recipient cells. The selective transfer of proteins and RNAs in the exosomal cargo represents an important mean of inter-cellular communication.

The exosomal microRNAs (miRNAs) can modulate the cellular microenvironment and exosomal RNA cargo selection is deregulated in pathological conditions. On the other hand, the mechanisms controlling specific RNA sorting into extracellular vesicles are still poorly understood. The selectivity of miRNA loading encodes the inter-cellular message carried by the exosome, but the mechanism of selectivity at the molecular level is a key question.

In this laboratory evidence has been recently provided on the mechanism allowing the loading in exosomes of a specific repertoire of miRNAs. This by identifying and determining the functional role of both a specific miRNAs motif and a specific interactor of it, i.e. the RNA-binding protein SYNCRIP (Synaptotagmin-binding Cytoplasmic RNA-Interacting Protein, hnRNP-Q or NSAP1) (1). SYNCRIP knock-down impairs sorting of miRNAs in exosomes. Furthermore, SYNCRIP directly binds to specific miRNAs enriched in exosomes sharing a common extra-seed sequence (hEXO motif). The hEXO motif

has a role in the exosome miRNA loading, since its embedment into a poorly-exported miRNA enhances the sorting of this molecule into exosomes.

On the other hand, a common putative CYTO motif, common to intracellular-enriched miRNAs, was previously characterized (2).

In this study, we demonstrated in hepatic cells that PCBP2 (Poly C-binding protein 2, αCP2 or hnRNPE2) is a protein interactor that specifically, and directly, binds to intracellular-retained miRNAs embedding a CYTO motif.

PCBP2 is localized in the intracellular compartment and its acts as a "retention factor". Its knock-down, indeed, determines the export of specific CYTO-miRNAs in exosomes.

Our results provide new insights into the knowledge of mechanisms controlling miRNA partition in the cell, characterizing a new negative regulator of exosomal loading.

INTRODUCTION

1. The Extracellular Vesicles (EV) and the growing role of the Exosomes

Extracellular vesicles (EVs) are vesicles composed of membrane whose release is evolutionally conserved in cells, ranging from prokaryotes to higher eukaryotes (2).

The secretion of EVs was initially described as a mean to eliminate unneeded compounds from the cell; now it is known that EVs are more than just waste carriers being able to exchange components between cells and to act as signaling vehicles in normal cell homeostatic processes or as a consequence of pathological developments (2; 3; 4; 5)

Based on their biogenesis, involving membrane-trafficking processes, EVs can be divided in two main categories: exosomes and microvesicles (6) (Fig.1).

Microvesicles, formerly called 'platelet dust', were first described as subcellular material originating from platelets in normal plasma and serum (7). They are characterized by a diameter of 50-1,000 nm and are generated by an outward budding of the plasma membrane and the subsequent fission and release in the extracellular space (8).

On the other hand, exosomes are intraluminal vesicles (ILVs) with a diameter of 30-100 nm. They are made up an inward budding of endosomal membrane during maturation of multivesicular endosomes (MVEs) and secreted upon fusion of MVEs with the cell surface (9; 5).

In recent years, exosomes have emerged as biological agents, essential in intercellular communication, with a therapeutic potential. In the era of nanomedicine, the study of mechanisms regulating the sorting of nucleic acids and proteins in exosomes are fundamental, as their changing content both in physiological and pathological conditions. This is necessary to exploit the therapeutic potential of exosomes in delivering drugs.

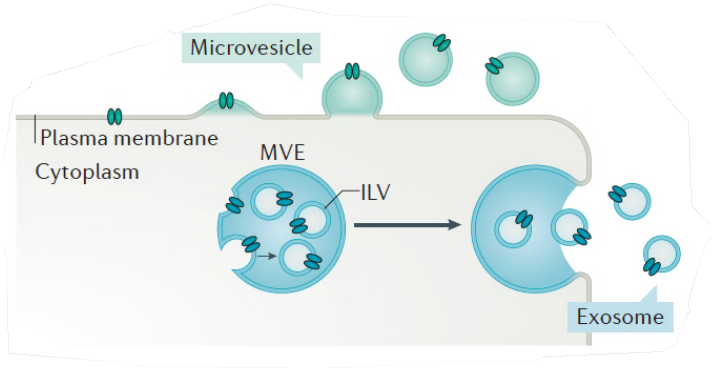

Fig.1 The Extracellular vesicles: the microvesicles are formed either by budding of the plasma membrane, instead the exosomes are release by the fusion of multivesicular endosomes (MVEs) with the plasma membrane (6) .

1.1 Biological properties of exosomes

Studies on exosomes' composition show that vesicles can carry various cargoes (proteins, lipids and nucleic acids). Their nature and abundance are cell-type-specific and often influenced by the physiological or pathological state of the donor cell (10; 11) (Fig. 2).

Protein and lipid configuration of exosomes depends on the different ways of biogenesis. They can be formed in two manners, so called ESCRT-dependent and ESCRT-independent pathways (Fig. 3).

In the first case, the Endosomal Sorting Complex Required for Transport (ESCRT) machinery is involved in the formation of ILVs and consists of four complexes associated proteins (12).

The former machinery acts in a stepwise manner: ESCRT-0 is responsible for clustering in a ubiquitin-dependent manner; ESCRT-I and ESCRT-II induce bud formation; ESCRT-III drives vesicle scission. Moreover, accessory proteins (especially the VPS4 ATPase) are involved in this mechanism to allow dissociation and recycling of ESCRT machinery. Also, Syntenin and ALIX (the ESCRT accessory protein ALG-2 interacting protein) are involved in linking between cargoes and ESCRT-III (13; 12).

The ESCRT-independent mechanisms can involve: lipids, tetraspanins or heat shock proteins.

In case of lipid involvement, ESCRT-independent mechanism of exosome biogenesis requires ceramide. In fact, it can allow the generation of membrane subdomains with a spontaneous negative curvature on the membranes. Alternatively, ceramide can be metabolized to sphingosine-1-phosphate to activate Gi protein-coupled sphingosine 1 phosphate receptor, essential for cargo sorting into exosomal ILVs (14).

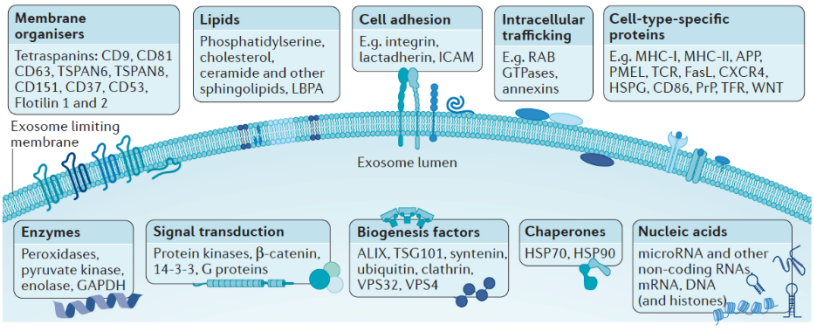

Fig.2 The exosomes composition: the exosomes can carry various cargoes including proteins, lipids and nucleic acids. The particular composition will directly affect the fate and function of extracellular vesicles, strengthening the importance of selective cargo-sorting mechanisms. Of note, depending on the cell type, exosomes will display a set of cell-type-specific proteins that account for their specific fates and functions (6) .

Proteins of the tetraspanin family (CD9, CD63, CD81 and CD82) can regulate ESCRT-independent endosomal sorting, too. Mechanistically, these proteins form clusters and dynamic membrane platforms with other tetraspanins or with different transmembrane and cytosolic proteins, probably acting in the formation of the microdomains that will bud (15). Recent structural analysis of tetraspanins revealed a cone-like structure with an intramembrane cavity that can accommodate cholesterol. Clustering of several tetraspanins could induce inward budding of the microdomain in which they are enriched (16). Finally, the heat shock proteins (HSP70, HSP90) turn out to be involved in sequestration of cytosolic proteins in to ILVs (17). In sum, both ESCRT-dependent and ESCRT-independent mechanisms operate in exosome biogenesis. Their contributions may vary depending on the cargoes, recruiting them, and the cell type.

In addition to the lipidic and proteic component linked to the biogenesis of exosomes, various other proteins are present on membrane vesicles. They are fundamental to drive mobilization of secretory MVBs and fusion of their limiting membrane with plasma membrane. In fact, the RAB family of small GTPase proteins (Rab4, Rab5, Rab7, Rab9, Rab11, Rab27, Rab35) controls different steps of intracellular vesicular trafficking: budding, mobility through cytoskeleton interaction, and docking

on the target compartment, leading to membrane fusion (18) (Fig. 3). Apart from proteins, exosomes also carry nucleic acids, including RNAs (mRNAs and non-coding RNAs) and DNA sequences (19; 20; 21; 22). The nucleic acids transfer plays a key role in cell-cell communication in many different contexts and pathologies.

The mechanisms involved in targeting nucleic acids to exosomes are so far elusive. Different machineries have been proposed to perform specific nucleic acid sorting: the ESCRT-II subcomplex acting as an RNA-binding complex (23); the tetraspanin-enriched microdomains sequestering RNA-binding proteins in the membrane subdomains (24; 25); the miRNA-induced silencing complex (miRISC) and protein argonaute 2 (AGO2), both mediating RNA-silencing processes (26).

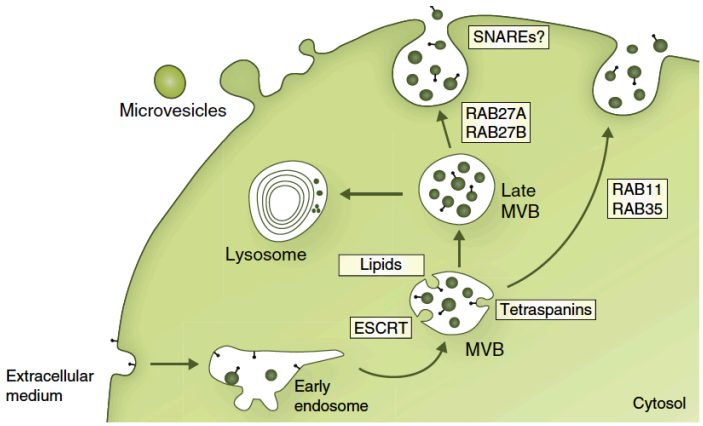

Fig.3 The intracellular machineries of exosome biogenesis and secretion. Exosomes are formed as ILVs by budding into early endosomes and MVBs. Several molecules are involved in the biogenesis of ILVs, such as the ESCRT machinery, lipids (such as ceramide) and the tetraspanins. The fate of MVBs can be either fusion with lysosomes or fusion with the PM, which allows the release of their content to the extracellular milieu. Several RAB proteins (RAB11, RAB27 and RAB35) have been shown to be involved in the transport of MVBs to the PM and in exosome secretion. In addition, SNAREs are probably involved in fusion of these MVBs with the PM (12).

1.2 Physiological and pathological functions of exosomes in cell-to-cell communication

Exosomes exert their effects on fundamental biological processes in different manner. They can directly activate cell surface receptors, merge their membrane contents into the recipient cell plasma membrane and deliver effectors (miRNAs, mRNAs, transcription factors, oncogenes and infectious particles into recipient cells) (27; 28).

The exosomes control fundamental cellular and biological functions (Fig 4).

They have been isolated from plasma, urine, tears, sweat, milk, seminal fluid, cerebrospinal fluid, participating in the maintenance of normal physiology (as stem cell maintenance, tissue repair, immune surveillance or blood coagulation) (29; 30; 25; 31).

Again, in addition to classical synaptic neurotransmission, neurons communicate via the secretion of exosomes that can contribute to a synaptic plasticity, too. It is demonstrated a greater glutamatergic activity with an increased release of extracellular vesicles containing neurotransmitter receptors from cortical neurons (32; 33).

Furthermore, immune responses can be regulated by the exosomes activity. Several mechanisms have been described for the suppression of the immune response: the exosomes can enhance the function of regulatory T cells, suppress natural killer (NK) and CD8+ cell activity, and inhibit monocyte differentiation into dendritic cells (DC) as well as DC maturation (34; 35). By contrast, the effects of immune activation can be mediated by exosome-promoted proliferation and survival of hematopoietic stem cells and the activation of monocytes, B cells and NK cells (36; 37).

In addition to their fundamental role in regulation biological processes, exosomes are often involved in the pathogenesis of the disease (Fig. 4).

The best pathologic understood role of exosomes is their involvement in tumoral biology. In fact, the tumor-derived exosomes (TDEs) are involved above all in processes for the formation of a pre-metastatic tumor niche and for the stimulation of tumor progression (38; 39). For instance, TDEs can

determine: neoplastic proliferation, angiogenesis, matrix remodeling via the secretion of matrix proteases, metastatic development and, finally, immune escape by modulating T cell activity (40; 41; 42; 43).

For this reason, TDEs have a fundamental role in many steps of tumor progression. Beyond cancers, exosomes have been implicated in the spread of numerous pathogens, including: HIV-1, via the horizontal transfer of C-C chemokine receptor 5 (CCR5), essential for viral cell entry; Epstein–Barr virus (EBV), via the transfer of viral miRNAs, repressing the expression of EBV target genes in non-infected cells; prions, via the selective delivery of PrP with specific modifications and glycoforms into neuronal cells (44; 45; 46). Finally, exosomes contribute to the local propagation of neurodegenerative disease, allowing longer-range communication within the central nervous system and affecting static neural networks located at a distance.

For instance, it has been shown that in the context of Alzheimer's disease, in which the pathologic β-amyloid peptides have been shown to be released in association with exosomes, contributing to the pathogenic deposition of amyloid-β in other parts of the brain (47). Similarly, the synuclein α protein has been detected inside the extracellular vesicles, providing a local propagation of

Parkinson's disease from enteric neurons to the brain and, so, to the superior cortical centers (48).

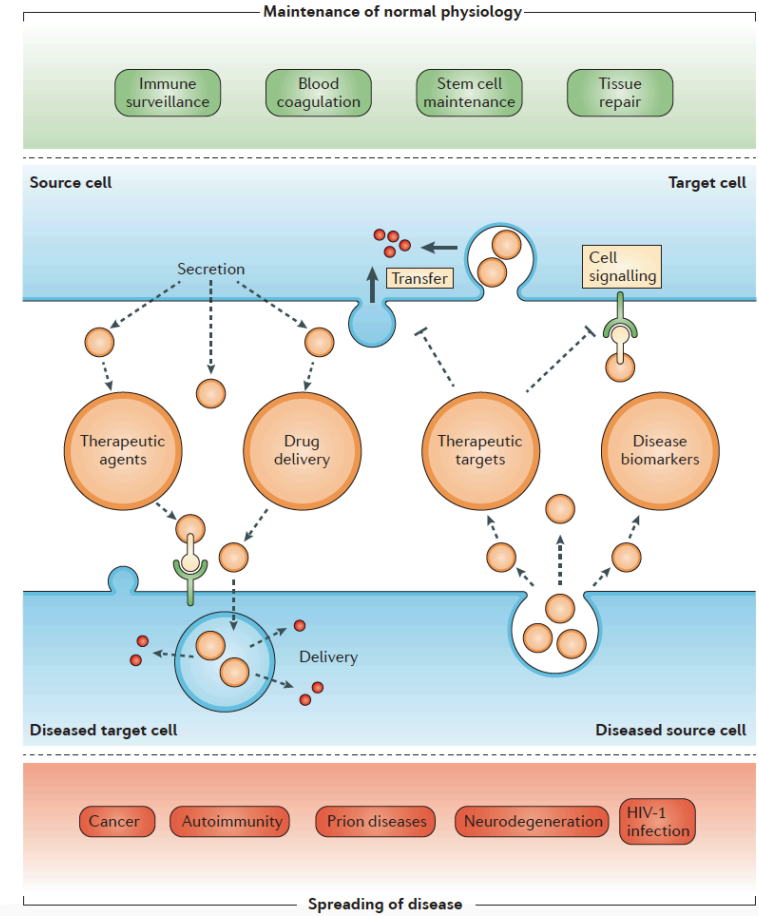

Fig.4 Roles of extracellular vesicles in normal physiology and disease pathogenesis (49).

2. Mechanisms controlling the selective loading of miRNAs in exosomes

The study of exosomal content through next generation sequencing (NGS) shows that the RNAs are the most abundant components in the vesicles. In particular, in addition to miRNAs and mRNAs, small ribosomal RNA (rRNAs) have been identified, together with structural RNAs (vRNAs, Y-RNAs and SRP-RNAs) and tRNAs, which are preferentially fragmented (50).

The RNA sorting into the exosomes is conceivably controlled by several mechanisms, still not fully understood.

With respect to mRNAs, a role for conserved zip-codes in the 3´ untranslated regions has been reported (51). Concerning miRNAs, different players can affect the sorting (Fig. 5). The neural sphingomyelinase 2 (nSMase2) is the first protein identified as involved in the loading of miRNAs into exosomes, although the mechanisms remain largely unclear. To date, the overexpression of nSMase2 seems to determine an increase in the number of exosomal miRNAs. On the other hand, there is a reduction of exported miRNAs in conditions of knock out nSMase2 (52).

Furthermore, the RNA-binding protein Y-box protein 1 (YBX1), located in the exosomes, is responsible for sorting of

some miRNAs and the other small noncoding RNA (tRNAs, Y-RNAs and Vault RNAs) in exosomes. YBX1 physically interacts with miR-233 and determines its packaging into exosomes (53; 54).

Moreover, with respect to sequence, miRNAs with 3-end rich of poly (U) are preferentially sorted into exosomes, while miRNAs with 3-end rich of poly (A) are preferentially intracellular (55).

Furthermore, through proteomic studies, AGO2 was identified in the exosomes. This suggests a correlation between AGO2 and the miRNA sorting. In fact, the knockout of AGO2 is responsible of decrease of the preferentially-exported miRNAs, such as miR-451, miR-150 and miR-142-3p (56).

Notably specific proteins, described in the next section, are known to bind specific elements of RNA sequence and to control the sorting of miRNAs into exosomes.

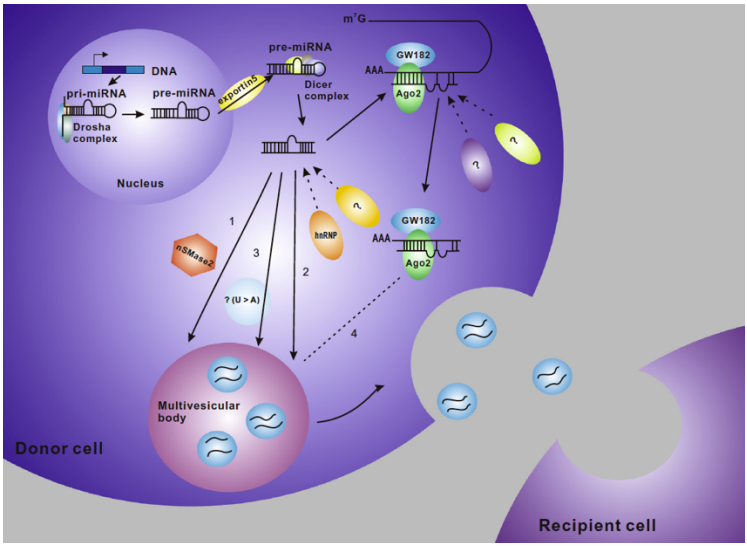

Fig.5 The sorting mechanism for exosomal miRNAs (57)**.**

2.1 Sequence-dependent miRNA sorting in exosomes

Currently, the research is focusing on the study of miRNA specific sequence responsible of loading into the exosomes.

There are only two miRNA motifs identified for the exosomal sorting: EXO- and hEXO- motif.

The first one is the “EXO Motif” (GGAG) identified by Villarroya-Beltri et al. in 2013 (58).

Analyzing miRNA profiles of primary T lymphoblasts and their exosomes, microarray assay shows that a lot of exosomal

miRNAs present a common sequence in the 3' half, so called EXO-motif.

Mutagenesis experiments show that EXO-motif is necessary for miRNA sorting. Furthermore, mass spectrometry identifies the Heterogeneous nuclear ribonucleoprotein A2B1 (hnRNPA2B1) in the exosomes. The sumoylated hnRNPA2B1 binds specifically the EXO-motif and is the regulator of EXO-miRNA sorting into exosomes.

The second one is the hEXO-motif (GGGCUG), identified by Santangelo et al. in 2016 (1), through analysis of miRNA profiles in murine hepatocytes and their exosomes.

The hEXO-motif is responsible of miRNA sorting only if is present in the extra seed. By biotin miRNA pull down, mass spectrometry and RIP analysis, the SYNCRIP (synaptotagmin-binding cytoplasmic RNA-interacting protein; also known as hnRNP Q or NSAP1) is found to interact directly on the hEXO-motif. The knockout of SYNCRIP is responsible of increase of hEXO-miRNAs in intracellular compartment. Also, in this case, mutagenesis experiments show that hEXO-motif is necessary for the SYNCRIP binding and, then, for miRNA sorting.

3. Role of Heterogeneous Nuclear Ribonucleoprotein (hnRNPs) in controlling miRNA partition

Heterogeneous nuclear ribonucleoproteins (hnRNPs) consist in a large family of RNA-binding proteins (RBPs). They are approximately 20 proteins. Most of them present a nuclear localization signal (NLS), predominantly localized in the nucleus. The hnRNP proteins frequently undergo post-translational modifications (methylation, phosphorylation, ubiquitination and sumoylation), with changes in biological activity and subcellular localization.

The hnRNPs are considered the key proteins in the nucleic acid metabolism. They have a role in the post-transcriptional processing and transport of RNA molecules (59).

Through the binding with specific sequences, hnRNPs regulate RNA processing, nucleo-cytoplasmic shuttling and maturation, intra-compartmental localization and turnover (60).

The hnRNPs are present in the cell and in extracellular space. These proteins are involved in the secretion of RNA in exosomes. The mechanism for binding and sorting is still unknown.

3.1 hnRNP A2B1: structure and functions

The hnRNP A2B1 is a ubiquitous protein by weight of 37 kDa. This protein consists of an N-terminal and a C-Terminal structural domain (Fig 6). In the N-terminal end there are two RNA recognition motif (RRM)-type RNA-binding domains, characterized by four β-sheets and two α-helices (βαββαβ) (59). In the C-terminal end, protein shares an arginine-glycine-rich subdomain that contains repeated arginine-glycine-glycine (RGG) sequences. The RGG region is an auxiliary domain. It is responsible for homologous and heterologous interactions with other hnRNPs, with capacity of binding RNA. For this reason, RGG-rich regions are considered an alternative RNA-binding domain. They are fundamental for the cellular localization of protein, too. In particular, RGG domain contains a nuclear localization sequence regulated by arginine methylation (61).
The hnRNP A2B1 is involved in mRNA translation and splicing. It plays an important role in oligodendrocytic and neuronal mRNA trafficking, binding an RNA transport signal present in the 3'UTR, called A2 response element (A2RE) (62; 63).
hnRNP A2B1 is involved in HIV RNA trafficking to the packaging sited by the binding to the A2RE sequences, too (64). Thanks to the prion-like domain, the hnRNP A2B1 can take part to the RNA granule assembly (cytoplasmatic riboprotein

granules consisting of nontranslated mRNA and translation repressors) (65).

Finally, sumoylated hnRNP A2B1 can carry the miRNA in the exosomes thanks to the ability of interacting with cytoskeletal proteins and binding directly the EXO motif (66).

3.2 SYNCRIP: structure and functions

SYNCRIP (hnRNP Q) is a conserved RNA-binding protein by the molecular weight of 73 kDa. The hnRNP Q presents three isoforms, called hnRNP Q1-Q3, according to alternative splicing events.

The protein contains three conserved RRM domains and an acid-rich domain in the N-terminal end. The α-helix acid-rich domain is essential for the interaction with the cytosine deaminase APOBEC1 (67). Instead, C-terminal end is unstructured, less conserved and it is important for the interaction with synaptotagmins (68) (Fig. 6).

Recent studies, based on the capacity of SYNCRIP to bind specific RNA targets, discover a non-canonical RNA-binding region in N-terminal end. The crystal structure of this region shows that the acid-rich domain is connected to the first RRM by a αββ sequence. The αββ sequence aligns the RRM1 and the N-terminal unit for RNA recognition (NURR), creating a

continuous RNA binding surface. The NURR domain, highly conserved, is essential for both recognition and binding to the hEXO-motif. The N-terminal NURR domain binds directly the GGCU/A sequence. The mutation in NURR domain causes the failure of SYNCRIP to bind the hEXO-miRNA and consequently the lack of its sorting in exosomes (69). The other RRM domains recognize a different range of RNA sequence: UACU and poly-A sequence (70; 71).

hnRNP Q regulates the mRNA editing, transport, translation and degradation, too (72; 73).

Finally, SYNCRIP is involved in neural and muscular development. In the nervous system, this protein takes part in the growth of neuromuscular junctions and in the nascent axons (74). For this reason, dysfunctions of hnRNP Q determine severe neuro-degenerative disorders and cardiomyopathies (75; 76; 77).

3.3 Poly-C Binding Protein 2: structure and functions

The Poly-C Binding Proteins 2 (PCBP2) is part of a subset of hnRNP E together with PCBP1, PCBP3 and PCBP4.

PCBP2, also called hnRNP E2 or αCP2, is characterized by high affinity for the polycytosine (polyC).

Like the other members of hnRNP E, PCBP2 presents three hnRNP K homology domains (KH domain): two of them are located near the N-terminal end; a third one is in the C-terminus. The structure of each KH domain is characterized by three β-strands, packed against three α-helices in a specific order (βααββα). A flexible loop (Gly-X-X-Gly) linking two α-helices in the KH core interacts with RNA. This interaction is mediated by a combination of electrostatic interactions, hydrogen binding and van der Waals contacts (78; 79). The hnRNP E2 carries two nuclear localization signals (NLS): the first one sequence (ten amino acids) is mapped between the KH1 and KH2 domains; the second NLS (twelve amino acids) is localized at the KH3 domain (80). For the NLS, αCP2 is predominantly localized to the nucleus. PCBP2 regulates gene expression at multiple levels, such as transcriptional regulation (81), mRNA stabilization and translation.

The hnRNP E2 can stabilize non-viral mRNA binding the C-rich element, present in 3'UTR. On the other hand, hnRNP E2 can stabilize viral mRNA binding the internal ribosome entry site (IRES) in the 5'UTR (82; 83). Furthermore, the PCBP2 binding to the IRES sequence in the IV domain of polio virus mRNA determinates the translational enhancement of mRNA (84; 85). Also, PCBP2 is an iron chaperone and contributes to ferritin iron loading (86). Finally, PCBP2 takes part in the miRNA

processing. This protein is associated with Argonaute 1 protein-containing complex with Dicer. *In vitro* studies suggest that cytosolic iron can regulate the multimerization of PCBP2, fundamental for interaction with pre-miRNA. PCBP2 can be multimerized when the cytosolic iron is low, binding pre-miRNAs and presenting them to Dicer for a more efficient miRNA processing. Meanwhile, an excess of cytosolic iron determines a non-binding of PCBP2 to the pre-miRNAs as well as the reduction of mature miRNAs production (87).

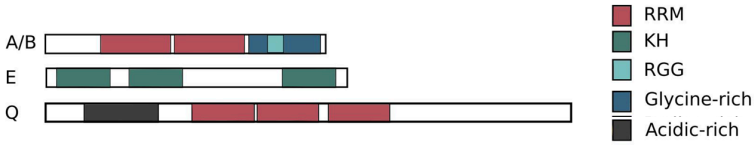

Fig.6 Some members of hnRNP family. The hnRNPs are named alphabetically from hnRNP A1 to hnRNP U. RRM RNA recognition motif, KH K-homology domain, RGG RNA-binding domain consisting of Arg-Gly-Gly repeats. Adapted from (59).

MATERIALS AND METHODS

1. Cell Culture Conditions

Nontumorigenic murine hepatocyte 3A cells (88) were grown at 37°C, in a humidified atmosphere with 5% CO2, in RPMI 1640 medium supplemented with 10% FBS (Gibco Life Technology), 50 ng/mL epidermal growth factor (EGF), 30 ng/mL insulin growth factor (IGF) II (PeproTech), 10 mg/mL insulin (Roche), and penicillin/streptomycin, on dishes coated with collagen I (Collagen I, Rat Tail; Gibco Life Technology). To collect hepatocyte exosomes, 80 × 106 cells were cultured for 72 hrs in RPMI-1640 supplemented with 10% FBS depleted of bovine exosomes by 70 minutes centrifugation at 100,000 × g (Beckman Optima L80; Beckman Coulter).

2. Exosome Purification

Extracellular vesicles were prepared according to International Society of Extracellular Vesicles (ISEV) recommendations (89). In particular to isolate exosomes, conditioned media (CM) from 12 150 mm plates each containing 13 million hepatocytes was collected after 72-hrs culture in complete medium containing exo-depleted FBS. Cell-conditioned media were centrifuged at 2,000 × g for 20 min to remove cells and then 20,000 × g for 1

hr to remove cell debris. Cleared supernatants were passed through 0.22 mm filter membranes, concentrated by VivaSpin 20 centrifugal filter device (Sartorius), ultracentrifuged in a SW32ti rotor at 100,000 rpm for 70 min, and finally resuspended in PBS.

To remove contaminant non-vesicular RNA-proteins (90), exosomes were treated with 100 mg/mL proteinase K (60 min) followed by heat inactivation of the protease; unprotected RNA was degraded by 15-min incubation with 2 mg/mL protease-free RNase A (Sigma-Aldrich) followed by addition of RNAsin RNase inhibitor (Promega).

To assess intravesicular localization of PCBP2, the exosomes were isolated with MagCapture (TM) Exosome Isolation Kit PS (FUJIFILM Wako) according to the manufacturer's instructions and were analyzed by western blot.

3. Biotin miRNA Pull-Down

Biotin miRNA pull-down experiments were performed on cytoplasmic extracts. Briefly, cells were lysed in hypotonic buffer (10 mM Tris-Cl [pH 7.5], 20 mM KCl, 1.5 mM MgCl2, 5 mM DTT, 0.5 mM EGTA, 5% glycerol, 0.5% NP40, and 40 U/mL RNAsin [Promega]) supplemented with protease inhibitors (Roche Applied Science). Lysates were incubated on ice for 30 min and then centrifuged at 13,000 rpm for 30 min at

4°C. Protein concentration was determined with Protein Assay Dye Reagent (Bio-Rad) based on the Bradford assay.

Samples (1 mg of proteins) were incubated for 1 hr at 4°C with 10 nmol synthetic single strand miRNA oligonucleotides containing a biotin modification attached to the 5' and via a spacer arm (Sigma-Aldrich) (Table 1) (91).

SoftLink Soft Release Avidin Resin beads (50 µL - Promega), previously blocked with 1 mg/mL yeast tRNA (Roche Applied Science), were added to reaction mixture for 90 min at 4°C, and then the beads were washed five times with 1 mL lysis buffer. Elution was for 5 min at room temperature with Laemly Buffer (containing 2-β mercaptoethanol and SDS).

Name	Oligonucleotides sequence
Biotin-miR-26b-3p	[Btn] CCU GUU CUC CAU UAC UUG GCU C
Biotin-miR-29b-3p	[Btn] UAG CAC CAU UUG AAA UCA GUG UU
Biotin-miR-96b-3p	[Btn] CAA UCA UGU GUA GUG CCA AUA U
Biotin-miR-155b-3p	[Btn] CUC CUA CCU GUU AGC AUU AAC
Biotin-miR-3470a	[Btn] UCA CUU UGU AGA CCA GGC UGG
Biotin-miR-29b-3p CYTO MUTATED	[Btn] UAG CGU UGC AUG AAA UCA GUG UU
Biotin-random	[Btn] CUU CAG UGA CAG CAC AUC GA
Biotin-polyA	[Btn] AAA AAA AAA AAA AAA AAA AAA

Table 1. Biotynilated RNA oligonucleotides used in pull down experiments

4. SDS-PAGE and Western Blotting

Cells were lysed in RIPA buffer (50 mM Tris-HCl pH 7.6, 150 mM NaCl, 0.5% sodium deoxycholate, 0.1% SDS, 1% NP40) containing freshly added cocktail protease inhibitors (cOmplete, EDTA-free Protease Inhibitor Cocktail; SigmaAldrich) and phosphatase inhibitors (5 mM EGTA pH 8.0; 50 mM sodium fluoride; 5 mM sodium orthovanadate). Lysates were incubated on ice for 20 min and then centrifuged at 13000 rpm for 30 min

at 4°C. Protein concentration was determined with Protein Assay Dye Reagent (Bio-Rad), based on the Bradford assay.

Samples (20 μg of proteins) were prepared in Laemly Buffer (containing 2-β mercaptoethanol and SDS) and were loaded on 10% acrylamide gels.

Gels were electrophoresed at 100 V in Running Buffer (25mM Tris, 190 mM glycine; 0.1% SDS) and then transferred to a nitrocellulose membrane (Pure Nitrocellulose Membrane 0.45 μm; Bio-Rad) at 100 V for 1 hr and 30 min in Transfer Buffer (50 mM Tris, 40 mM glycine; 0.1% SDS; 20% Methanol).

Blots were blocked in 5% non-fat milk prepared in TBS-Tween (10mM Tris-HCl pH 7.5; 150mM NaCl; 0.05% Tween 20) and incubated overnight with the primary antibody (α-PCBP2 cod. AV40568 – Sigma Aldrich; α-SYNCRIP cod. MAB11004 – Millipore α-Alix cod.2171S – Cell Signaling; α-Tubulin cod. SC-5286 – Santa Cruz).

Then blots were incubated with HRP-conjugated species-specific secondary antibodies (Goat Anti-Mouse IgG (H+L)-HRP Conjugated 170-6516 or Goat Anti-Rabbit IgG (H+L)-HRP Conjugated 172-1019) followed by enhanced chemiluminescence reaction (Clarity Max ECL Substrate and Clarity Western ECL Substrate – Bio-Rad) and the signal was revealed through autoradiography X-ray film.

5. RNA Extraction, RT-PCR and Real-Time qPCR

Total RNA from cells and exosomes was isolated by Qiazol and the miRNeasy Mini Kit and (QIAGEN) following the manufacturer's protocols. RNA purity was assessed by spectrophotometric measure of optical density 260 (OD_{260})/OD_{280} ≈ 2 and OD_{260}/OD_{230} >1.8 with a Nanodrop 2000c Spectrophotometer (Thermo Fisher Scientific).

Intracellular and exosomal total RNA (150 ng) was reverse transcribed with the MystiCQ microRNA cDNA Synthesis Mix (Sigma Aldrich) according to the manufacturer's protocol. Diluted (1:10) cDNA samples were used for qPCR in a total volume of 10 μL using GoTaq qPCR Master Mix (Promega) and the reaction were carried out in Bio-Rad-iQ-iCycler.

The cycling condition were: 95°C for 3 min, followed by 40 cycles at 95°C for 10 sec 57°C for 30 sec, then the temperature was raised from 65°C to 95°C with 0.5°C increase step for 0.5 seconds. The melting temperature is variable according to the sequence of oligonucleotides. The sequence of primer used are listed in Table 2 and 3. The small RNA U6 was used for normalization of miRNA relative quantities in both cellular and exosomal preparations.

The results were analysed with Manager Software (Bio-Rad) and calculates with the ΔC(t) method.

miRNA	**Primer sequence**	**Tm (ºC)**
mmu-miR-26b-3p	CCT GTT CTC CAT TAC TTG GCT C	62
mmu-miR-29b-3p	TAG CAC CAT TTG AAA TCA GTG TT	61.5
mmu-miR-96-3p	CAA TCA TGT GTA GTG CCA ATA T	57
mmu-miR-155- 3p	CTC CTA CCT GTT AGC ATT AAC	57
mmu-miR-194-2-3p	CCA GTG GGG CTG CTG TTA TCT G	63.9
mmu-miR-328- 3p	GGC CCT CTC TGC CCT TC	60
mmu-miR-365-2-5p	GAC TTT CAG GGG CAG CTG	58
mmu-miR-3470a	TCA CTT TGT AGA CCA GGC TG	61

Table 2. Primers for miRNAs qPCR analysis.

Name	Primer sequence	Tm (ºC)
PCBP2	*For* ACACCGGATTCAGTGGCA *Rev* TTGATTTTGGCGCCTTGACG	58 58
Rpl32	*For* AAGCGAAACTGGCGGAAAC *Rev* TAACCGATGTTGGGCATCAG	57 58
Rnu6	*For* TCGCTTCGGCAGCACATA *Rev* ACGAATTTGCGTGTCATCCT	56 56

Table 3. Primers for RT-qPCR analysis.

6. Co-Immunoprecipitation

Cells were lised with IP Lysis Buffer (150 mM NaCl, 50 mM Tris-HCl pH 7.5, 2 mM EDTA, 1% TRITON-X100 and 10% glycerol) plus containing freshly added cocktail protease inhibitors (cOmplete, EDTA-free Protease Inhibitor Cocktail; SigmaAldrich) and phosphatase inhibitors (5 mM EGTA pH 8.0; 50 mM sodium fluoride; 5 mM sodium orthovanadate). Lysates were incubated on ice for 1h and then centrifuged at 13000 rpm for 30 min at 4°C. Protein concentration was determined with Protein Assay Dye Reagent (Bio-Rad), based on the Bradford assay.

2 mg of proteins (one for the specific antibody and one for the specie-specific corresponding IgG) were precleared adding 40 µL of Protein A Sepharose for 3 hrs at 4°C in a total volume of 1 ml of IP Lysis Buffer in rotation.

Then, Protein A Sepharose was removed by centrifugation and the extract were incubated with 5 µg of specific antibody α-PCBP2 (cod. RN025P - MBL) or Normal Rabbit IgG (cod. 12-370 - Millipore) as negative control, to proceed with immunoprecipitation at 4°C overnight.
Immuno-complexes were collected adding 50 µL of Protein A Sepharose for 3 hrs at °C in rotation.
The immunoprecipitated proteins were washed trice with Net Gel Buffer (150 mM NaCl, 50 mM Tris-HCl pH 7.5, 1mM EDTA, 0.1% NP40 and 0.25% gelatin).
Finally, immunoprecipitated proteins were separated from Protein A Sepharose adding 50 µL of Laemly Buffer 2X. Samples were boiled at 95°C for 5 min, beads were eliminated by centrifugation and half of each sample was loaded on polyacrilammide gel and analysed by Western Blotting.

7. UV Cross-Linking RIP

In UV cross-linking RIP, hepatocytes were washed twice with PBS and subjected to UV cross-linking (one-time irradiation at 800 mJ/cm2 in 254 nm Stratalinker - Stratagene 2400, Stratagene).
Cells were then lysed in 10 mM HEPES (pH 7.3), 20 mM KCl, 2 mM MgCl2, 0.5 mM EGTA, 1 mM EDTA, 1 mM DTT, 40

U/mL RNAsin inhibitor, 0.1% SDS, 0.5% sodium deoxycholate, and 0.5% NP40 at 4°C for 10 min. After that, lysates were centrifuged at 13,000 rpm for 30 min at 4°C. Protein concentration was determined with Protein Assay Dye Reagent (Bio-Rad) based on the Bradford assay.

1 mg protein aliquots (one for the specific antibody and one for the specie-specific corresponding IgG) were diluted in NT2 buffer (50 mM Tris-HCl pH 7.4, 150 mM NaCl, 1 mM $MgCl_2$, 0.05% NP40) plus protease inhibitor and RNAsin inhibitor and precleared with 15 µL protein A/G Dynabeads (Invitrogen) for 30 min in rotation.

Pre-cleared proteins were centrifuged at 13,000 rpm for 10 sec and the supernatant was incubated over night at 4°C in rotation with 5 µg of specific antibody (α-PCBP2 cod. RN025P – MBL; α-SYNCRIP cod. 05-1517 – Millipore) or IgG (Normal Rabbit IgG cod. 12-370 – Millipore; Normal Mouse IgG cod. 12-371– Millipore) as negative control, to proceed with immunoprecipitation.

Immunoprecipitated complexes were collected by incubation with 20 µL Dynabeads (Protein A Dynabeads for PCBP2 immunoprecipitation; Protein G Dynabeads for SYNCRIP immunoprecipitation; Invitrogen) for 3 hrs at 4°C in rotation. The complex beads-proteins were collected and, before

washing, 100 µL of the supernatant of the IgG samples were collected and stored as Input sample.

The samples were washed 5 times with the Denaturing Wash Buffer (500 mM LiCl, 0.2% SDS and 0.1% Sodium deoxycholate) (92; 93) plus protease inhibitor to allow only the detection of direct interactions. Coimmunoprecipitated miRNAs were extracted using Qiazol and the miRNeasy kit. qPCR analysis was performed with GoTaq qPCR Master Mix (Promega) and miRNA fold enrichment in immunoprecipitated samples were expressed as IP/IgG.

8. shRNA Silencing

Stable PCBP2 knockdowns were achieved through infection with shRNAs cloned in pSUPER retro puro retroviral vector (Oligoengine).

Viral supernatants were collected 48 hrs after transfection of 293 gp packaging cells, filtered (0.45 mm), and added to hepatocytes. At 48 hrs post-infection, selection was performed with 2 µg/mL puromycin for at least 1 week before analysis. The sequence of shRNA scramble used as control was previously described (94). The sequences of shRNA oligos used for cloning are reported in Table 4. The stable PCBP2 knockdowns and the

control cellular line are called respectively 3A shPCBP2 and 3A shCTR.

Name	Sequence
PCBP2	*S* GATCCCCGAGCAGACCCATCCATAATT TCAAGAGAATTATGGATGGGTCTGCTC TTTTTA *As* AGCTTAAAAAGAGCAGACCCATCCATA ATTCTCTTGAAATTATGGATGGGTCTG CTCGGG
Scramble	*S* GATCCCCGCGAAAGATGATAAGCTAAT TCAAGAGATTAGCTTATCATCTTTCGCT TTTTA *As* AGCTTAAAAAGCGAAAGATGATAAGC TAATCTCTTGAATTAGCTTATCATCTTT CGCGGG

Table 4. Oligos for shRNA cloning in pSUPER.retro.puro vector.

9. Statistical Analysis

For the qRT-PCR analysis, statistical differences were assessed with the one-tailed paired Student's t-test using GraphPad Prism Version 6 (GraphPad Software). Data are presented as mean ± SD, and p values < 0.05 were considered statistically significant.

AIM OF THE WORK

Recently, great advances were made in the knowledge about exosomal composition and function in pathological and physiological conditions. Evidence showed that the miRNAs' sorting into the exosomes is well-regulated. A growing number of proteins was identified to be involved in this process, but sequence-specific mechanisms and RNA-binding regulators responsible of the control of miRNA partition are still largely unknown.

Our previous results indicated that exosomal microRNAs presented a common sequence called hEXO-motif. This sequence was responsible of miRNAs sorting in to the exosomes. Furthermore, the hnRNP SYNCRIP (hnRNPQ) was identified as a direct interactor of hEXO-motif, by pull down experiment followed by a mass spectrometry analysis.

We found that a SYNCRIP knock-down determined a reduced sorting of hEXO-miRNAs.

Starting from these observations, we aimed to investigate the role of other proteins in the molecular machinery determining miRNAs loading into the exosome or the intracellular retention. In this frame, we here described the identification of another hnRNP, the RNA-binding protein PCBP2 (hnRNPE2) as a negative regulator of exosomal miRNA loading.

RESULTS

1. PCBP2 is an interactor of hCYTO-miRNAs

Starting from the analysis of a small RNA sequencing, Santangelo and colleagues previously investigated in hepatocytes on the partition of miRNAs in intracellular and/or EV compartments (1). Published results highlighted the existence of specific repertoires of miRNAs enriched in exosomes (called hEXO-miRNAs) or in the intracellular compartment (called hCYTO-miRNAs). In particular, 69 hCYTO-miRNAs were identified, with a fold enrichment [FE] ≤ -1.5 and a false discovery rate [FDR] ≤ 0.10 (Table 5), on the other hand 126 miRNAs were enriched in the exosomes, with a [FE] ≥ 1.5 and FDR] ≤ 0.10 (1). The hEXO - motif, found causal for miRNA export in exosomes (1), was discovered thanks to a comparison of the sequences of exosomal miRNAs, using Improbizer (95). However, the same approach applied to the analysis of intracellular retained miRNA sequences did not allowed the identification of common motifs. Nevertheless, through a simple sequence comparison, we here identified a subset of miRNAs sharing a putative CL motif (A/UC/ACAUU/G) (Fig.7A and Table 6), previously identified by Villarroya-Beltri et al. in 2013 (58).

Aiming to identify proteins able to bind miRNAs embedding the CL-motif (and possibly involved in controlling miRNA retention), we incubated the hepatocyte extracts with streptavidin beads coated with the biotinylated hCYTO-miRNA miR-29b-3p as probe and, as a negative control, a biotinylated random sequence (see Methods). Then, the pulled-down proteins were subjected to mass spectrometry through Q-EXACTIVE PLUS -Orbitrap Mass Spectrometer (in collaboration with Montaldo C., INMI Lazzaro Spallanzani, IRCCS, Rome). Thanks to a Gene Onthology analysis, different RNA-binding proteins were identified (data not shown). Among the RNA-binding proteins precipitated with miR-29b-3p and not with the random sequence, we focused on PCBP2. In fact, as shown in Fig. 7B, PCBP2 binding to different hCYTO-miRNAs was validated by pull-down experiments and successive western blot analysis. For these experiments, the poly-A sequence was used as a positive control while the random sequence was used as a negative control. MiRNAs embedding a putative CL-motif, such as miR-26b-3p, miR-29b-3p, miR-96-3p and miR-155-3p were used as probes (Fig 7B). These analyses demonstrated that PCBP2 is an interactor of different hCYTO-miRNAs sharing a putative CL-motif.

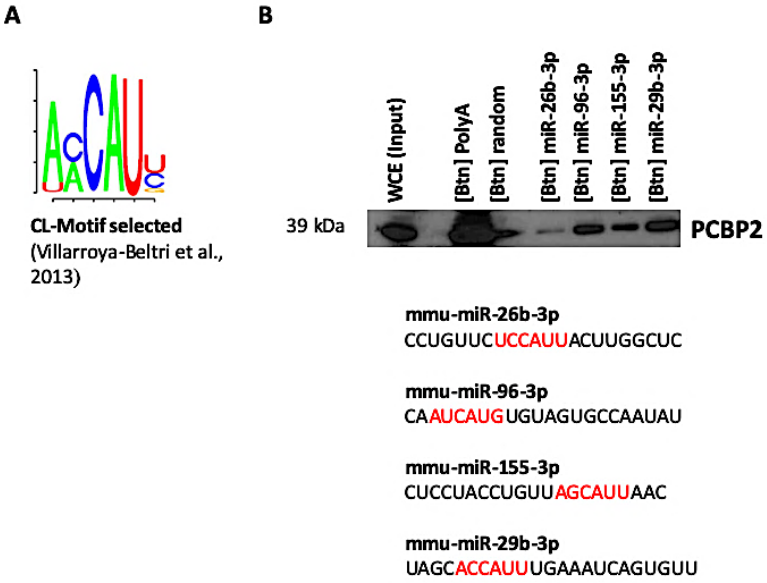

Fig 7. Identification of PCBP2 as bound to hCYTO-miRNAs.

A. CL-motif identified by Villarroya-Beltri et al., 2013 and used for our analysis (58).

B. Western blot analysis for PCBP2 in samples derived by miRNA pull-downs performed with cellular extracts of murine hepatocytes and the indicated biotinylated [Btn] miRNAs, selected for our analysis as embedding a putative CL-motif (indicated in red). Poly(A) was used as positive control, while random sequence was used as a negative control. WCE, whole cellular extract.

2. PCBP2 binding to the CL-motif is direct and sequence specific

To get further inside on the interaction between PCBP2 and CL-embedding miRNAs, we performed RIP experiments (Fig.8A). In particular, to identify only the direct protein-RNA interactions, RIPs were carried out by denaturing wash protocol after UV cross-linking (according to McHugh et al., 2015; Battistelli et al., 2016).

By RIP assays, PCBP2 was found to directly bind to hCYTO-miRNAs previously analysed by pull-down experiments, such as miR-26b-3p, miR-29b-3p, miR-96-3p and miR-155-3p. In these experiments, positive control of PCBP2 binding was miR-328-3p (according to Eiring et al., 2010 (96)). On the other hand, miR-365-2-5p was used as a negative control, embedding the hEXO motif but no CL-motifs.

A

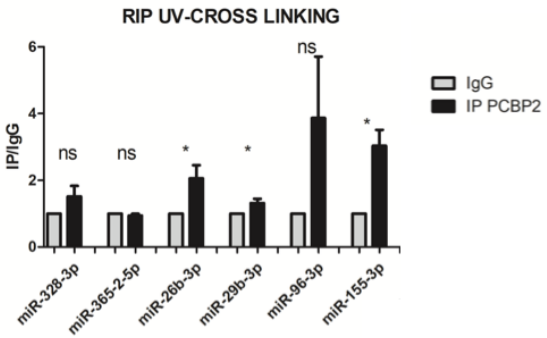

B

mmu-miR-29b-3p
UAGCACCAUUUGAAAUCAGUGUU

mmu-miR-29b-3p CYTO MUTATED
UAGCGUUGCAUGAAAUCAGUGUU

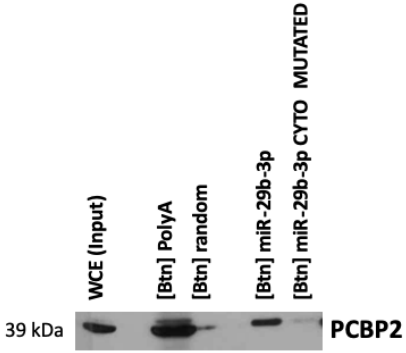

Fig 8. PCBP2 binding to the CL-motif is direct and sequence specific

A. RNA immunoprecipitation experiments with anti-PCBP2 antibody (or IgG as control) performed on cellular lysates. The levels of the indicated miRNAs in immunoprecipitated samples were determined by qRT-PCR and reported as ratio between IP/IgG. Data are means ± SD of four independent experiments, and statistically significant differences are reported (*$p < 0.05$; ns, no significance).

B. Western blot analysis for PCBP2 in samples derived from miRNA pull-downs performed with cellular extracts of murine hepatocytes and the indicated biotinylated [Btn] miRNAs (lower panel). [Btn]Poly A, [Btn] Random sequence, [Btn] miR-29b-3p and Btn] miR-29b-3 CYTO MUTATED (upper panel). WCE, whole cellular extract.

These analyses demonstrated that PCBP2 directly binds to a subset of hCYTO-miRNAs sharing a CL-motif.

We further analyzed the PCBP2 binding capacity when the CL-motif sequence is mutated. An artificial miR-29-3p was generated by mutation of all the six bases of the CL sequence (A/UC/ACAUU/G was changed in GUUGCA; the mutant form was called miR29-3p-CYTO MUTATED).

We performed a pull-down experiment using [Btn]miR-29b-3p, [Btn]miR-29b-3p CYTO MUTATED and as negative control a random sequence. As shown in Fig. 8B, the next western blot analysis demonstrated that the PCBP2 capacity of binding to hCYTO-miRNA was drastically reduced when the specific CL-motif sequence is mutated.

Overall, these results demonstrated that the PCBP2 binding to the CL-motif is direct and sequence specific.

3. PCBP2 has a role in controlling hCYTO-miRNAs retention

To assess the possible functional role of PCBP2 in miRNA partition, we in first investigated on PCBP2 localization in intracellular or exosomal compartments.

According to International Society of Extracellular Vesicles (ISEV) recommendations (89), conditioned media (CM) from 13 million hepatocytes was collected after 72-hrs culture to isolate exosomes and was centrifuged to remove cells (2,000 × g for 20 min) and cell debris (20,000 × g for 1 hr). Then, the exosomes were isolated with MagCapture (TM) Exosome Isolation Kit (see details in Methods).

Western blot analysis on both cellular an exosomal protein extracts demonstrated that PCBP2 is an intracellular protein. Indeed, it does not colocalize with the exosome specific marker Alix (13), nor with SYNCRIP, previously validated as able to be embedded in these vesicles (1) (Fig. 9A).

Next, we assessed the effect of PCPBP2 silencing with respect to miRNA sorting, aiming to investigate on its possible functional role in miRNAs retention.

Thus, short hairpin RNAs (shRNAs) for PCBP2 silencing and a scramble sequence (Table 4) were cloned in the pSUPER retro puro retroviral vector (Oligoengine). Then, 293 gp packaging

cells were transfected with the correspondent pSUPER-0 (empty vector as CTR.) or the pSUPER-PCBP2 vector. Viral supernatants were collected 48 hrs after transfection and hepatocytes were infected with the retroviruses expressing the short hairpin RNA against PCBP2 or a scrambled sequence as control. At 48 hrs post-infection, stable 3A shCTR and shPCBP2 cell lines were obtained by selection with 2 μg/mL puromycin for at least 1 week. As shown in fig 8B, western blot and qRT-PCR analysis demonstrated that PCBP2 levels were significantly reduced in cells infected with the retrovirus targeting its transcript (Fig. 9B)

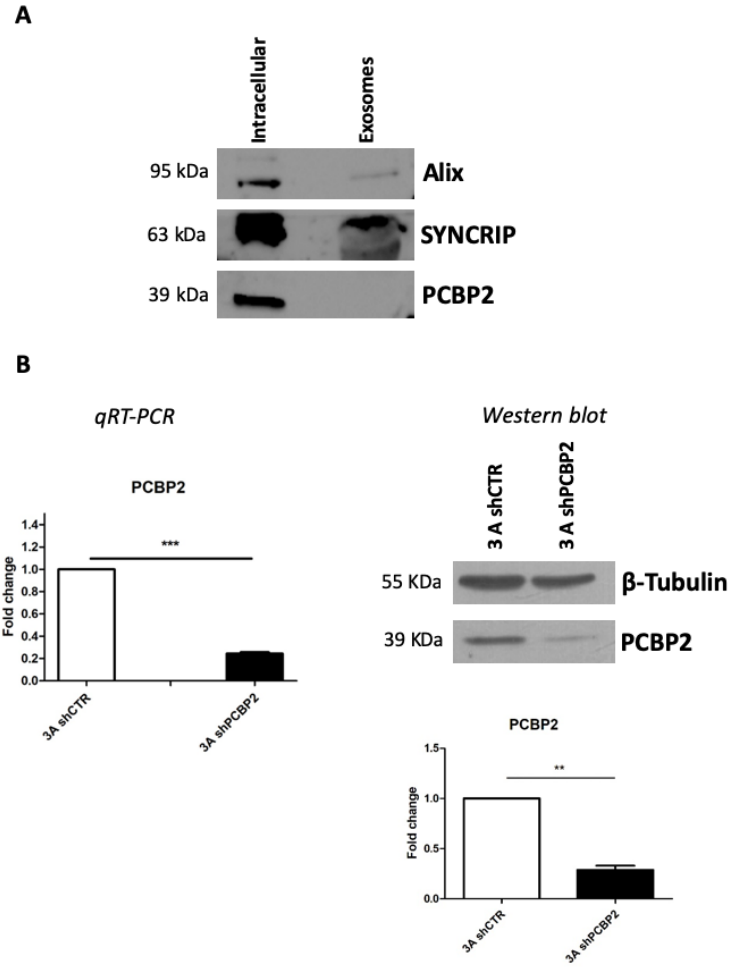
A
Intracellular
Exosomes
95 kDa
Alix
63 kDa
SYNCRIP
39 kDa
PCBP2
B
qRT-PCR
PCBP2
Fold change
1.4
1.2
1.0
0.8
0.6
0.4
0.2
0.0
***
3A shCTR
3A shPCBP2
Western blot
3 A shCTR
3 A shPCBP2
55 KDa
β-Tubulin
39 KDa
PCBP2
PCBP2
Fold change
1.5
1.0
0.5
0.0
**
3A shCTR
3A shPCBP2

Fig 9. PCBP2 localization and silencing.
A. Western blot analysis of exosomal and intracellular extracts for PCBP2, SYNCRIP and the exosomal marker Alix. The reported experiment is representative of three independent ones.
B. PCBP2 protein and mRNA levels in cytoplasmic extracts of PCBP2-silenced (shPCBP2) and shCTR hepatocytes. β-tubulin has been used as loading control. The densitometry analysis (lower left panel) was made quantified the protein levels using ImageJ software. Data are means ± SD of three independent experiments, and statistically significant differences are reported (***$p < 0.001$; ** $p < 0.01$).

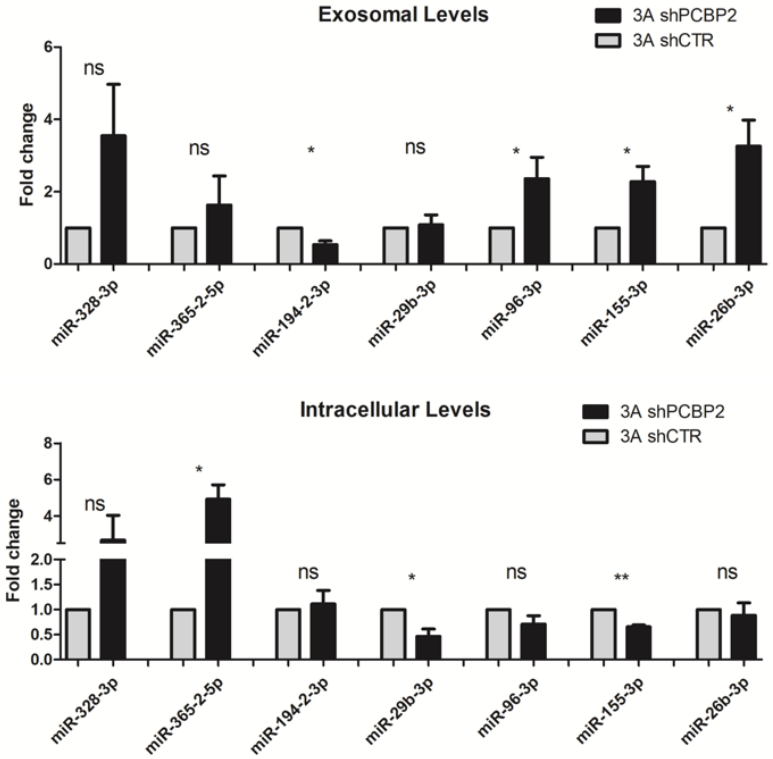

Fig 10. Role of PCBP2 in hCYTO-miRNAs retention.
qRT-PCR analysis of exosomal (upper panel) and intracellular (lower panel) levels of selected miRNAs in shPCBP2 compared to shCTR control. The values are calculated by the ΔΔCt method, normalized to small nuclear RNA (snRNA) U6 levels in exosomes or cells, expressed as fold enrichment and shown as mean ± SD. Statistically significant differences are reported for five independent experiments (* $p < 0.05$; ** $p < 0.01$; ns, no significance).

As showed in fig 10 upper panel, the comparison of microRNA levels in exosomes produced respectively by stably silenced PCBP2 cells and control cells confirmed that hCYTO-miRNAs (miR-26b-3p, miR-155-3p, miR-96-3p, and miR-29b-3p) were more represented in the exosomes, once PCBP2 was interfered. The miRNAs used as control were the hEXO-miRNAs miR-365-2-5p and miR-194-2-3p (1).

Thus, PCBP2 knock-down correlates to the hCYTO-miRNAs loading in to the exosomes, suggesting that PCBP2 may act as a retention factor.

4. PCBP2 and SYNCRIP display different sequence-specific binding

We found by a simple sequence comparison that some miRNAs, such as miR-3470a, embed both the putative CL-motif A/UC/ACAUU/G and the hEXO motif GGCU (this latter) previously found causal to the loading in exosomes and bound by SYNCRIP (1). This observation prompted us to assess whether PCBP2 and SYNCRIP binding capacity to miRNA sequences could be antagonistic in determining the partition outcome.

The selective binding capacity of both proteins was assessed by RNA-immunoprecipitation experiments after UV-crosslinking.

In PCBP2 immunoprecipitated samples miR-29b-3p, embedding a CL-motif, and miR-3470, with both CL- and hEXO-motifs, were found enriched. Conversely, PCBP2 did not directly bind to miR-365, characterized as a hEXO-motif embedding-miRNA (Fig. 11 A left panel). Furthermore, PCBP2 silencing impacted on the export in exosomes of the miR-3470, resulting in a further loading of this exosomal miRNA (Fig. 11 B). On the other hand, SYNCRIP did not bind to miR-29-3p, that has only the CL-motif, while it was able to directly bind to the hEXO-miR-365 and to the miR-3470, showing both motifs (Fig. 11 A right panel). Furthermore, Santangelo and colleagues (1) demonstrated that knock-down of SYNCRIP did not caused an exosomal loading of the intracellular enriched (and CL-motif embedding) miR-29-3p, only affecting the export of hEXO-miRs, such as miR-3470 and miR-365.

Interestingly, co-immunoprecipitation (Co-IP) assays did not show the interaction between SYNCRIP and PCBP2. As shown in Fig 11 C, Western blot analysis of co-immunoprecipated samples demonstrated that PCBP2 and SYNCRIP do not interact (note that the co-immunoprecipitation was performed in presence of RNAsi inhibitors, thus the possible assembly of a RNA-mediated protein-protein complex was excluded).

Overall, these data indicate that the two proteins display sequence-specific capacity in regulate the partition in the cell of

selected miRNAs. However, with respect to miRNAs with both sequence signals of retention and export, both proteins can bind them, maybe antagonistically (thus, PCBP2 knock-down could render available to SYNCRIP-mediated export a reservoir of intracellular miRNAs).

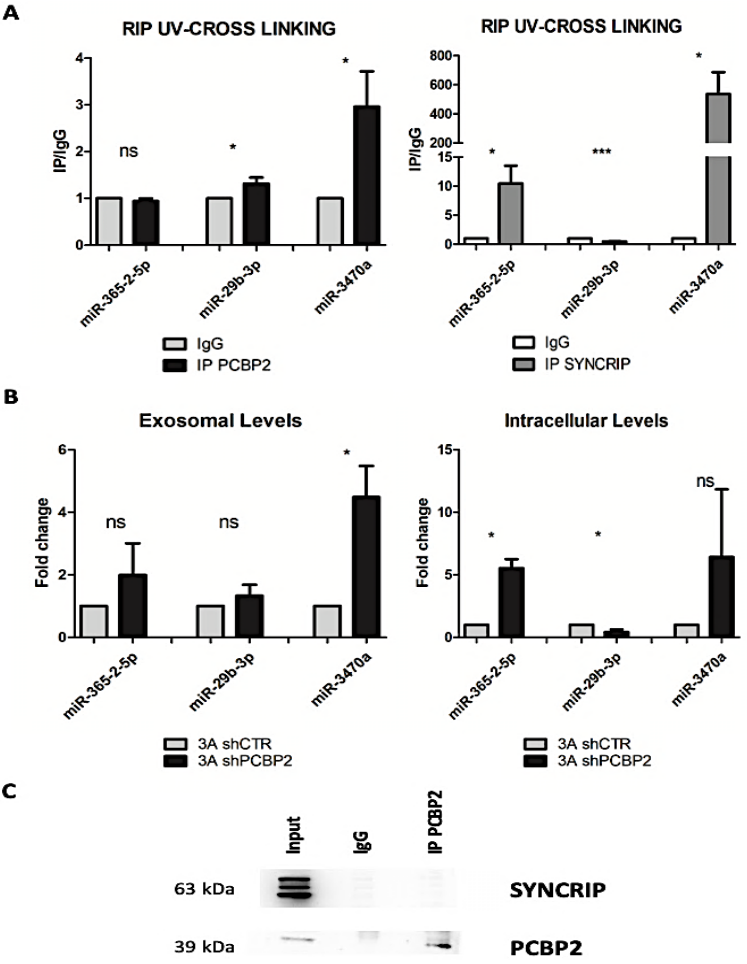
A
RIP UV-CROSS LINKING
IP/IgG
ns
*
*
miR-365-2-5p
miR-29b-3p
miR-3470a
IgG
IP PCBP2
RIP UV-CROSS LINKING
IP/IgG
*
***
*
miR-365-2-5p
miR-29b-3p
miR-3470a
IgG
IP SYNCRIP
B
Exosomal Levels
Fold change
ns
ns
*
miR-365-2-5p
miR-29b-3p
miR-3470a
3A shCTR
3A shPCBP2
Intracellular Levels
Fold change
*
*
ns
miR-365-2-5p
miR-29b-3p
miR-3470a
3A shCTR
3A shPCBP2
C
Input
IgG
IP PCBP2
63 kDa
SYNCRIP
39 kDa
PCBP2

Fig 11. PCBP2 and SYNCRIP display different sequence-specific binding.
A. RNA immunoprecipitation experiments with anti-PCBP2 antibody (left panel) and anti-SYNCRIP (right panel) (or IgG as control) performed on cellular lysates. The levels of the indicated miRNAs in immunoprecipitated samples were determined by qRT-PCR and reported as ratio between IP/IgG. Data are means ± SD of three independent experiments, and statistically significant differences are reported (*$p < 0.05$; ***$p < 0.001$; ns, no significance)
B. qRT-PCR analysis of exosomal (right panel) and intracellular (left panel) levels of selected miRNAs in shPCBP2 compared to shCTR control. The values are calculated by the ΔΔCt method, normalized to small nuclear RNA (snRNA) U6 levels in exosomes or cells, expressed as fold enrichment and shown as mean ± SD. Statistically significant differences are reported for five independent experiments (* $p < 0.05$; ns, no significance).
C. Immunoprecipitation of PCBP2 in murine hepatocyte cells with rabbit polyclonal anti-PCBP2 was analyzed for Western Blotting with anti-PCBP2 and anti-SYNCRIP antibody. The control immunoprecipitation was performed with Normal rabbit antiserum (IgG). The reported experiment is representative of three independent ones.

DISCUSSION AND CONCLUSION

In our study, we investigated on the role played by the RNA binding protein PCBP2 in controlling miRNAs partition in the cell.

The RNA Binding Protein PCBP2 is a member of hnRNP E family. The protein is characterized by its involvement in the stabilization of viral and non-viral mRNA (82; 83; 84; 85), it has been described associated with Argonaute 1 protein-containing complex with Dicer and it is also involved in the miRNAs maturations (87).

Concerning microRNA partition, while current knowledge points to a key role for the exosome-mediated transfer in cell-to-cell communication, the processes controlling the selective compartmentalization between cell and EV, in physiology and disease, are still largely uncharacterized. Recent evidence highlighted the loading in exosomes of miRNAs in dependence of different RNA-binding proteins. In particular, a functional role in miRNA loading was attributed to the RBP SYNCRIP: the knock-down of this protein in hepatocytes impaired the exosomal loading of some exosome-enriched microRNAs. Moreover, SYNCRIP binds directly, through the NURR domain (69), to exported miRNAs characterized to embed a short hEXO

motif. Notably, the insertion of this sequence in a normally cell-retained miRNA induced its exosomal export, highlighting the functional role of this sequence motif.

It's conceivable that a multiprotein machinery dynamically governs both the EVs sorting and the intracellular retention of specific subsets of miRNAs. Interestingly, in lymphocytes Villaroya and colleagues highlighted that intracellular miRNAs were enriched in specific sequence determinants, called (CL)-motifs (58).

Here, the RBP Poly-C-binding protein 2 is identified in the hepatocyte as a component of the machinery controlling miRNA partition between cell and EVs. RNA immunoprecipitation after UV cross-linking demonstrated that this protein directly binds to some miRNAs embedding the CL-motif (A/UC/ACAUU/G) and RNA pull down by using as probe an intracellular miRNA (miR-29b) mutated in this sequence proved the specificity of binding. Moreover, PCBP2 knock-down allows the EVs loading of specific intracellular-enriched microRNAs, this implying a functional role for this protein in retention of specific molecules.

Finally, as depicted in Fig 12, our data revealed that PCBP2 and SYNCRIP binding to miRNAs is sequence-specific (panels A and B). In the case of miRNAs with both the motifs (e.g. miR-3470), while RIP analysis demonstrated that both the proteins

could interact to these RNA molecules, co-immunoprecipitation assays highlighted that SYNCRIP and PCBP2 do not form a complex, this conceivably implying a mutually exclusive binding (see panel C). When PCBP2 levels are lower, it's conceivable that a larger fraction of miRNAs is available for SYNCRIP-mediated export (Fig 12 panel C).

However, further studies are necessary to clarify the mechanisms controlling PCBP2 and SYNCRIP function in the cell as well as to approach the systematic characterization of the riboprotein machinery that governs the exosome-mediated pivotal mechanism of cell-to-cell communication.

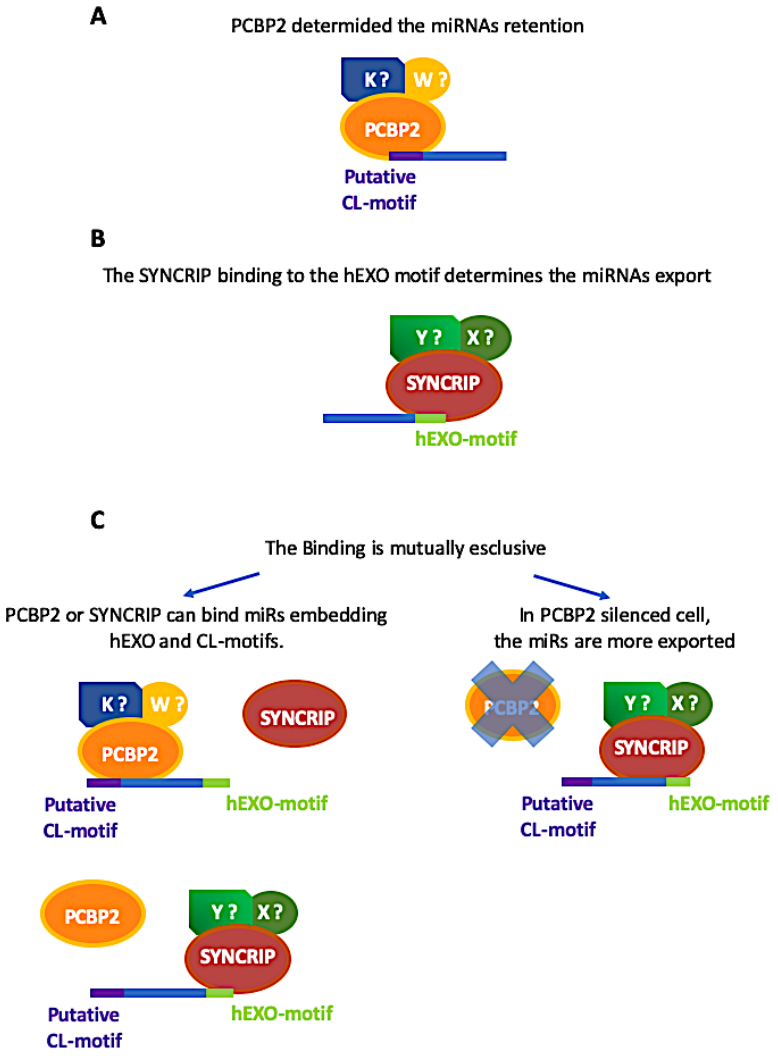
A
PCBP2 determided the miRNAs retention
K?
W?
PCBP2
Putative
CL-motif
B
The SYNCRIP binding to the hEXO motif determines the miRNAs export
Y?
X?
SYNCRIP
hEXO-motif
C
The Binding is mutually esclusive
PCBP2 or SYNCRIP can bind miRs embedding
hEXO and CL-motifs.
In PCBP2 silenced cell,
the miRs are more exported
K?
W?
PCBP2
SYNCRIP
Putative
CL-motif
hEXO-motif
PCBP2
Y?
X?
SYNCRIP
Putative
CL-motif
hEXO-motif
PCBP2
Y?
X?
SYNCRIP
Putative
CL-motif
hEXO-motif

Fig 12. Proposed molecular model.
A. miRNAs with a putative CL-motif were intracellular thank to PCBP2 binding
B. SYNCRIP was responsible of hEXO-miRNAs sorting in to the exosomes (1) .
C. Both SYNCRIP and PCBP2 can bind miRNAs with both CL-motif and hEXO-motif. Probably, the balance between them can determine miRNA fate and the RNA fractions available to SYNCRIP are exported. In PCBP2 knock down condition, a larger fraction of miRNAs is available to SYNCRIP –mediated sorting into the exosomes.

APPENDIX

hCYTO-miRNAs with Exo versus Cell FE <=1.5			
miRNA	**log2 FE**	**FE**	**P value**
mmu-miR-181b-1-3p	-4,84	-28,64	3,70E-10
mmu-miR-155-3p	-4,65	-25,10	0,003842355
mmu-miR-6539	-4,64	-24,89	1,23E-11
mmu-let-7c-1-3p	-3,54	-11,60	0,017624529
mmu-miR-26a-2-3p	-3,48	-11,18	6,80E-05
mmu-miR-1291	-3,32	-10,00	0,004779382
mmu-miR-31-3p	-3,06	-8,34	6,82E-05
mmu-miR-96-3p	-3,06	-8,32	0,002266478
mmu-miR-30d-3p	-2,87	-7,33	2,77E-10
mmu-miR-98-3p	-2,86	-7,25	9,43E-05
mmu-miR-770-5p	-2,84	-7,15	0,008352633
mmu-miR-182-3p	-2,68	-6,41	0,000800133
mmu-miR-24-1-5p	-2,66	-6,32	0,000133799
mmu-miR-450b-5p	-2,59	-6,04	1,89E-16
mmu-miR-677-5p	-2,47	-5,53	0,010238144
mmu-miR-374c-3p	-2,39	-5,23	0,000258931
mmu-miR-339-3p	-2,35	-5,10	0,009557318
mmu-miR-152-5p	-2,34	-5,07	3,75E-05
mmu-miR-30b-5p	-2,34	-5,05	0,00098675
mmu-miR-6914-3p	-2,22	-4,64	0,026323071
mmu-miR-582-5p	-2,20	-4,59	0,000778831
mmu-miR-3963	-2,19	-4,57	0,00058735
mmu-miR-26a-1-3p	-2,11	-4,30	0,011252497
mmu-miR-24-2-5p	-2,07	-4,19	0,002501594
mmu-miR-148b-5p	-1,97	-3,91	0,005718163
mmu-miR-27b-5p	-1,94	-3,83	9,05E-05
mmu-miR-27a-5p	-1,93	-3,82	0,001836188

mmu-miR-301a-5p	-1,92	-3,79	0,002181934
mmu-miR-181a-1-3p	-1,92	-3,79	0,000252485
mmu-miR-296-5p	-1,89	-3,71	7,33E-05
mmu-miR-700-5p	-1,87	-3,67	0,011509892
mmu-miR-702-3p	-1,84	-3,59	0,000537268
mmu-miR-582-3p	-1,83	-3,55	0,000308816
mmu-miR-331-3p	-1,82	-3,53	0,0189538
mmu-miR-450a-5p	-1,82	-3,53	5,86E-08
mmu-let-7f-1-3p	-1,82	-3,52	4,84E-05
mmu-miR-181c-5p	-1,77	-3,42	0,000529543
mmu-miR-200a-5p	-1,75	-3,37	0,010390178
mmu-miR-148b-3p	-1,74	-3,34	7,26E-09
mmu-miR-326-3p	-1,70	-3,26	0,002570155
mmu-miR-29c-3p	-1,70	-3,25	0,020579101
mmu-let-7f-2-3p	-1,66	-3,17	0,011523613
mmu-miR-30c-1-3p	-1,65	-3,14	0,008079124
mmu-miR-21a-5p	-1,64	-3,12	3,46E-18
mmu-miR-183-3p	-1,56	-2,95	0,012416158
mmu-miR-129-2-3p	-1,55	-2,94	0,007045177
mmu-miR-181c-3p	-1,54	-2,92	0,001633009
mmu-miR-3102-3p.2-3p	-1,54	-2,90	0,016431251
mmu-miR-872-3p	-1,54	-2,90	0,019395233
mmu-miR-92a-1-5p	-1,53	-2,88	0,014796053
mmu-miR-15b-3p	-1,51	-2,84	0,00531211
mmu-miR-744-3p	-1,45	-2,74	0,022527563
mmu-miR-330-5p	-1,44	-2,72	0,001492934
mmu-miR-192-3p	-1,42	-2,67	0,029469126
mmu-miR-26b-3p	-1,40	-2,64	0,019022386
mmu-miR-16-2-3p	-1,38	-2,61	0,010300709
mmu-miR-3109-3p	-1,36	-2,57	0,019703042
mmu-miR-542-3p	-1,36	-2,56	0,000203214

mmu-miR-26b-5p	-1,34	-2,53	2,17E-08
mmu-miR-194-5p	-1,34	-2,53	0,016321071
mmu-let-7b-3p	-1,22	-2,32	0,000848952
mmu-miR-192-5p	-1,19	-2,29	0,007244431
mmu-miR-676-5p	-1,19	-2,28	0,027157968
mmu-miR-301a-3p	-1,16	-2,23	0,006545763
mmu-miR-872-5p	-1,15	-2,22	2,83E-05
mmu-miR-301b-3p	-1,15	-2,22	0,001583586
mmu-miR-1843b-5p	-1,11	-2,15	0,023827271
mmu-miR-26a-5p	-0,97	-1,96	0,010963296
mmu-miR-674-3p	-0,76	-1,70	0,023655557

Table 5. hCYTO-miRNAs with a fold enrichment [FE] ≤ -1.5 and a false discovery rate [FDR] ≤ 0.10 from Santangelo et al., 2016.

mmu-miR-194-5p	UGUAACAGCAACUCCAUGUGGA
mmu-miR-26b-3p	CCUGUUCUCCAUUACUUGGCUC
mmu-miR-181a-1-3p	ACCAUCGACCGUUGAUUGUACC
mmu-miR-96-3p	CAAUCAUGUGUAGUGCCAAUAU
mmu-miR-155-3p	CUCCUACCUGUUAGCAUUAAC
mmu-miR-15b-3p	CGAAUCAUUAUUUGCUGCUCUA
mmu-miR-148b-3p	UCAGUGCAUCACAGAACUUUGU
mmu-miR-31-3p-5p	UGCUAUGCCAACAUAUUGCCAUC

Table 6. hCYTO-miRNAs with CL-motif (red) selected for our analysis.

REFERENCES

1. **Santangelo L, Giurato G, Cicchini C, Montaldo C, Mancone C, Tarallo R and Tripodi M.** The RNA-Binding Protein SYNCRIP Is a Component of the Hepatocyte Exosomal Machinery Controlling MicroRNA Sorting. . *Cell Reports, 17(3), 799-808. doi. 2016.*

2. **Yáñez-Mó M, Siljander PR, Andreu Z, Zavec AB, Borràs FE, Buzas EI, Buzas K, Casal E, Cappello F, Carvalho J, Colás E, Cordeiro-da Silva A, Fais S, Falcon-Perez JM, Ghobrial IM, Giebel B, Gimona M et al..** Biological properties of extracellular vesicles and their physiological functions. *J Extracell Vesicles. 2015 May 14;4:27066. doi: 10.3402/jev.v4.27066. eCollection 2015.*

3. **Colombo M, Raposo G and Théry C.** Biogenesis, secretion, and intercellular interactions of exosomes and other extracellular vesicles. . *Annu Rev Cell Dev Biol. 2014;30:255-89. doi: 10.1146/annurev-cellbio-101512-122326. Epub 2014 Aug21.*

4. **Lo Cicero A, Stahl PD and Raposo G.** Extracellular vesicles shuffling intercellular messages: for good or for bad. . *Curr. Opin. Cell Biol. 35,69–77 (2015).*

5. **Pan BT, Teng K, Wu C, Ada M and Johnstone RM.** Electron microscopic evidence for externalization of the transferrin receptor in vesicular form in sheep reticulocytes. . *J. Cell Biol. 101,942–948 (1985).*

6. **van Niel G, D'Angelo G, Raposo G.** Shedding light on the cell biology of extracellular vesicles. . *Nat Rev Mol Cell Biol. 2018 Apr;19(4): 213228. doi: 10.1038/nrm.2017.125. Epub 2018 Jan 17.*

7. **P., Wolf.** The nature and significance of platelet products in human plasma. . *Br. J. Haematol. 13, 269–288 (1967).*

8. **Tricario C, Clancy J and De Souza-Schorey C.** Biology and biogenesis of shed microvesicles. *Small GTPases 1–13 (2016).*

9. **Harding C, Heuser J and Stahl P.** Endocytosis and intracellular processing of transferrin and colloidalgold

transferrin in rat reticulocytes: demonstration of a pathway for receptor shedding. . *Eur. J. Cell Biol. 35, 256–263 (1984).*
10. **Kalra H, Drummen GP and Mathivanan S.** Focus on extracellular vesicles: introducing the next small big thing. *Int. J. Mol. Sci. 17, 170 (2016).*
11. **Minciacchi VR, Freeman MR and Di Vizio D.** Extracellular vesicles in cancer: exosomes, microvesicles and the emerging role of large oncosomes. . *Semin. Cell Dev. Biol. 40, 41–51 (2015).* .
12. **Kowal J, Tkach M and Thery C.** Biogenesis and secretion of exosomes. *Cell Biology 2014, 29: 116-125* .
13. **Baietti MF, Zhang Z, Mortier E, Melchior A, Degeest G, Geeraerts A, Ivarsson Y, Depoortere F, Coomans C, Vermeiren E, Zimmermann P and David G.** Syndecan-syntenin-ALIX regulates the biogenesis of exosomes. *Nat. Cell Biol. 14, 677–685 (2012).*
14. **Kajimoto T, Okada T, Miya S, Zhang L and Nakamura S.** Ongoing activation of sphingosine 1-phosphate receptors mediates maturation of exosomal multivesicular endosomes. . *Nat. Commun. 4, 2712 (2013).*
15. **Charrin S, Jouannet S, Boucheix C and Rubinstein E.** Tetraspanins at a glance. *J. Cell Sci. 127, 3641–3648 (2014).*
16. **Zimmerman B, Kelly B, McMillan BJ, Seegar TCM, Dror RO, Kruse AC and Blacklow SC.** Crystal structure of a full-length human tetraspanin reveals a cholesterol-binding pocket. *Cell 167, 1041–1051.e11 (2016).*
17. **Geminard C, De Gassart A, Blanc L and Vidal M.** Degradation of AP2 during reticulocyte maturation enhances binding of hsc70 and Alix to a common site on TfR for sorting into exosomes. *Traffic 5, 181–193 (2004).*
18. **H., Stenmark.** Rab GTPases as coordinators of vesicle traffic. *Nat Rev Mol Cell Biol 2009, 10:513-525.*
19. **Valadi, H. et al.** Exosome-mediated transfer of mRNAs and microRNAs is a novel mechanism of genetic exchange between cells. . *Nat. Cell Biol. 9, 654–659 (2007).*

20. **Nolte-'t Hoen EN, Buermans HP, Waasdorp M, Stoorvogel W, Wauben MH and 't Hoen PA.** Deep sequencing of RNA from immune cell-derived vesicles uncovers the selective incorporation of small non-coding RNA biotypes with potential regulatory functions. *Nucleic Acids Res. 40, 9272–9285 (2012).*
21. **Thakur BK, Zhang H, Becker A, Matei I, Huang Y, Costa-Silva B, Zheng Y, Hoshino A, Brazier H, Xiang J, Williams C, Rodriguez-Barrueco R, Silva JM, Zhang W, Hearn S, Elemento O, Paknejad N, Manova-Todorova K, Welte K, Bromberg J et l..** Double-stranded DNA in exosomes: a novel biomarker in cancer detection. *Cell Res. 24, 766–769 (2014).*
22. **Kahlert C, Melo SA, Protopopov A, Tang J, Seth S, Koch M, Zhang J, Weitz J, Chin L, Futreal A and Kalluri R.** Identification of double-stranded genomic DNA spanning all chromosomes with mutated KRAS and p53 DNA in the serum exosomes of patients with pancreatic cancer. *J. Biol. Chem. 289, 3869–3875 (2014).*
23. **D., Irion U and St Johnston.** bicoid RNA localization requires specific binding of an endosomal sorting complex. . *Nature 445, 554–558 (2007).*
24. **Perez-Hernandez D, Gutiérrez-Vázquez C, Jorge I, López-Martín S, Ursa A, Sánchez-Madrid F, Vázquez J and Yáñez-Mó M.** The intracellular interactome of tetraspanin-enriched microdomains reveals their function as sorting machineries toward exosomes. *J. Biol. Chem. 288, 11649–11661 (2013).*
25. **Raposo G, Nijman HW, Stoorvogel W, Liejendekker R, Harding CV, Melief CJ and Geuze HJ.** B lymphocytes secrete antigenpresenting vesicles. *J. Exp. Med. 183, 1161–1172 (1996).*
26. **Gibbings DJ, Ciaudo C, Erhardt M and Voinnet O.** Multivesicular bodies associate with components of miRNA effector complexes and modulate miRNA activity. . *Nature Cell Biol. 11, 1143–1149 (2009).*

27. **Lee Y, El Andaloussi S and Wood MJA.** Exosomes and microvesicles: extracellular vesicles for genetic information transfer and gene therapy. *Hum. Mol. Genet. 21, R125–R134 (2012).*
28. **Valadi H, Ekström K, Bossios A, Sjöstrand M, Lee JJ and Lötvall JO.** Exosome-mediated transfer of mRNAs and microRNAs is a novel mechanism of genetic exchange between cells. *Nature Cell Biol. 9, 654–659 (2007).*
29. **Ratajczak J, Miekus K, Kucia M, Zhang J, Reca R, Dvorak P and Ratajczak MZ.** Embryonic stem cell-derived microvesicles reprogram hematopoietic progenitors: evidence for horizontal transfer of mRNA and protein delivery. *Leukemia 20, 847–856 (2006).*
30. **Gatti S, Bruno S, Deregibus MC, Sordi A, Cantaluppi V, Tetta C and Camussi G.** Microvesicles derived from human adult mesenchymal stem cells protect against ischaemia-reperfusion-induced acute and chronic kidney injury. *Nephrol. Dial. Transplant. 26, 1474–1483 (2011).*
31. **Del Conde I, Shrimpton CN, Thiagarajan P and López JA.** Tissue-factor-bearing microvesicles arise from lipid rafts and fuse with activated platelets to initiate coagulation. . *Blood 106, 1604–1611 (2005).*
32. **Chivet M, Hemming F, Pernet-Gallay K, Fraboulet S and Sadoul R.** Emerging role of neuronal exosomes in the central nervous system. . *Front. Physiol. 3, 145 (2012).*
33. **Lachenal G, Pernet-Gallay K, Chivet M, Hemming FJ, Belly A, Bodon G, Blot B, Haase G, Goldberg Y and Sadoul R.** Release of exosomes from differentiated neurons and its regulation by synaptic glutamatergic activity. *Mol. Cell. Neurosci. 46, 409–418 (2011).*
34. **Clayton A, Mitchell JP, Court J, Mason MD and Tabi Z.** Human tumor-derived exosomes selectively impair lymphocyte responses to interleukin-2. *Cancer Res. 67, 7458–7466 (2007).*
35. **Clayton A, Mitchell JP, Court J, Linnane S, Mason MD and Tabi Z.** Human tumor-derived exosomes down-modulate NKG2D expression. *J. Immunol. 180, 7249–7258 (2008).*

36. **Simhadri VR, Reiners KS, Hansen HP, Topolar D, Simhadri VL, Nohroudi K, Kufer TA, Engert A and Pogge von Strandmann E.** Dendritic cells release HLA-B-associated transcript-3 positive exosomes to regulate natural killer function. *PLoS ONE 3, e3377 (2008).*
37. **Baj-Krzyworzeka M, Majka M, Pratico D, Ratajczak J, Vilaire G, Kijowski J, Reca R, Janowska-Wieczorek A and Ratajczak MZ.** Platelet-derived microparticles stimulate proliferation, survival, adhesion, and chemotaxis of hematopoietic cells. *Exp. Hematol. 30, 450–459 (2002).*
38. **A., Rak J and Guha.** Extracellular vesicles — vehicles that spread cancer genes. . *Bioessays 34, 489–497 (2012).*
39. **Peinado H, Alecˇković M, Lavotshkin S, Matei I, Costa-Silva B, Moreno-Bueno G, Hergueta-Redondo M, Williams C, García-Santos G, Ghajar CM, Nitadori-Hoshino A, Hoffman C, Badal K, Garcia BA, Callahan MK, Yuan J, Martins VR, Skog J, Kaplan RN, et al..** Melanoma exosomes educate bone marrow progenitor cells toward a pro-metastatic phenotype through MET. *Nature Med. 18, 883–891 (2012).*
40. **Al-Nedawi K, Meehan B, Micallef J, Lhotak V, May L Guha A and Rak J.** Intercellular transfer of the oncogenic receptor EGFRvIII by microvesicles derived from tumour cells. *Nature Cell Biol. 10, 619–624 (2008).*
41. **Skog J, Würdinger T, van Rijn S, Meijer DH, Gainche L, Sena-Esteves M, Curry WT Jr, Carter BS, Krichevsky AM and Breakefield XO.** Glioblastoma microvesicles transport RNA and proteins that promote tumour growth and provide diagnostic biomarkers. *Nature Cell Biol. 10, 1470–1476 (2008).*
42. **Al-Nedawi, K., Meehan B, Kerbel RS, Allison AC and Rak J.** Endothelial expression of autocrine VEGF upon the uptake of tumor-derived microvesicles containing oncogenic EGFR. . *Proc.Natl Acad. Sci. USA 106, 3794–3799 (2009).*
43. **Wieckowski, E. U et al.** Tumor-derived microvesicles promote regulatory T cell expansion and induce apoptosis in tumor-reactive activated CD8+ T lymphocytes. *J. Immunol. 183, 3720–3730 (2009).*

44. **Mack M, Kleinschmidt A, Brühl H, Klier C, Nelson PJ, Cihak J, Plachý J, Stangassinger M, Erfle V and Schlöndorff D.** Transfer of the chemokine receptor CCR5 between cells by membrane-derived microparticles: a mechanism for cellular human immunodeficiency virus 1 infection. *Nature Med. 6, 769–775 (2000).*
45. **Vella LJ, Sharples RA, Lawson VA, Masters CL, Cappai R and Hill AF.** Packaging of prions into exosomes is associated with a novel pathway of PrP processing. *J. Pathol. 211, 582–590 (2007).*
46. **Pegtel DM, Cosmopoulos K, Thorley-Lawson DA, van Eijndhoven MA, Hopmans ES, Lindenberg JL, de Gruijl TD, Würdinger T and Middeldorp JM.** Functional delivery of viral miRNAs via exosomes. *Proc. Natl Acad. Sci. USA 107, 6328–6333 (2010).*
47. **Bellingham SA, Guo BB, Coleman BM and Hill AF.** Exosomes: vehicles for the transfer of toxic proteins associated with neurodegenerative diseases? . *Front. Physiol. 3, 124 (2012).*
48. **Harding C, Heuser J and Stahl P.** Endocytosis and intracellular processing of transferrin and colloidal gold-transferrin in rat reticulocytes: demonstration of a pathway for receptor shedding. *Eur. J. Cell Biol. 35, 256–263 (1984).*
49. **Andaloussi SEL, Mäger I,Breakefield XO and Wood MJA.** Extracellular vesicles: biology and emerging therapeutic opportunities. *Send to Nat Rev Drug Discov. 2013 May;12(5):347-57. doi: 10.1038/nrd3978. Epub 2013 Apr 15.*
50. **Nolte-'t Hoen EN, Buermans HP, Waasdorp M, Stoorvogel W, Wauben MH and t Hoen PA.** Deep sequencing of RNA from immune cell-derived vesiclesuncovers the selective incorporation of small non-coding RNA biotypes withpotential regulatory functions. *Nucleic Acids Res 2012;40(18):9272-85.*
51. **Bolukbasi MF, Mizrak A, Ozdener GB, Madlener S, Ströbel T, Erkan EP, Fan JB, Breakefield XO and Saydam**

O. miR-1289 and "zipcode"-like sequence enrich mRNAs in microvesicles. *Mol. Ther. Nucleic Acids 1, e10 (2012).*
52. **Kosaka N, Iguchi H, Hagiwara K, Yoshioka Y, Takeshita F and Ochiya T.** Neutral sphingomyelinase 2 (nSMase2)-dependent exosomal transfer of angiogenic microRNAs regulate cancer cell metastasis. . *J Biol Chem 2013;288:10849–59. .*
53. **Shurtleff MJ1, Temoche-Diaz MM, Karfilis KV, Ri S and Schekman R.** Y-box protein 1 is required to sort microRNAs into exosomes in cells and in a cell-free reaction. *Elife. 2016 Aug 25;5. pii: e19276. doi: 10.7554/eLife.19276.*
54. **Shurtleff MJ, Yao J, Qin Y, Nottingham RM, Temoche-Diaz MM, Schekman R and Lambowitz AM7.** Broad role for YBX1 in defining the small noncoding RNA composition of exosomes. *Proc Natl Acad Sci U S A. 2017 Oct 24;114(43):E8987-E8995. doi: 10.1073/pnas.1712108114. Epub 2017 Oct 10.*
55. **Koppers-Lalic D, Hackenberg M, Bijnsdorp IV, van Eijndhoven MA, Sadek P, Sie D, et al.** Nontemplated nucleotide additions distinguish the small RNA composition in cells from exosomes. . *Cell Rep 2014;8:1649–58.*
56. **Guduric-Fuchs J, O'Connor A, Camp B, O'Neill CL, Medina RJ and Simpson DA.** Selective extracellular vesicle-mediated export of an overlapping set of microRNAs from multiple cell types. . *BMC Genomics 2012;13:357.*
57. **Zhang J, Li S, Li L, Li M, Guo C, Yao J and Mi S.** Exosome and Exosomal MicroRNA: Trafficking, Sorting, and Function. *Genomics Proteomics Bioinformatics 13 (2015) 17–24.*
58. **Villarroya-Beltri C, Gutierrez-Vazquez C, Sanchez-Cabo F, Perez-Hernandez D, Vazquez J, Martin-Cofreces N, et al.** Sumoylated hnRNPA2B1 controls the sorting of miRNAs into exosomes through binding to specific motifs. *Nat Commun 2013;4:2980.*
59. **Geuens T, Bouhy D and Timmerman V.** The hnRNP family: insights into their role in health and disease. *Hum Genet.*

2016 Aug;135(8):851-67. doi: 10.1007/s00439-016-1683-5. Epub 2016 May 23.
60. **Statello L, Maugeri M, Garre E, Nawaz M, Wahlgren J, Papadimitriou A, Lundqvist C, Lindfors L, Collén A, Sunnerhagen P, Ragusa M, Purrello M, Di Pietro C, Tigue N and Valadi H.** Identification of RNA-binding proteins in exosomes capable of interacting with different types of RNA: RBP-facilitated transport of RNAs into exosomes. *PLoS One. 2018 Apr 24;13(4):e0195969. doi: 10.1371/journal.pone.0195969. eCollection 2018.*
61. **Nichols RC, Wang XW, Tang J, Hamilton BJ, High FA, Herschman HR and Rigby WFC.** The RGG Domain in hnRNP A2 affects subcellular localization. *Exp Cell Res. 2000 May 1;256(2):522-32.*
62. **Shan J, Moran-Jones K, Munro TP et al .** Binding of an RNA trafficking response element to heterogeneous nuclear ribonucleoproteins A1 and A2. J. *Biol Chem 275:38286–38295. doi:10.1074/jbc.M007642200.*
63. **Hoek KS, Kidd GJ, Carson JH and Smith R.** hnRNP A2 selectively binds the cytoplasmic transport sequence of myelin basic protein mRNA. *Biochemistry. 1998 May 12;37(19):7021-9.*
64. **Bériault V, Clément JF, Lévesque K, Lebel C, Yong X, Chabot B, Cohen EA, Cochrane AW, Rigby WF and Mouland AJ.** A late role for the association of hnRNP A2 with the HIV-1 hnRNP A2 response elements in genomic RNA, Gag, and Vpr localization. *J Biol Chem. 2004 Oct 15;279(42):44141-53. Epub 2004 Aug 3.*
65. **Kim HJ, Kim NC, Wang YD, Scarborough EA, Moore J, Diaz Z, MacLea KS, Freibaum B, Li S, Molliex A, Kanagaraj AP, Carter R, Boylan KB, Wojtas AM, Rademakers R, Pinkus JL, Greenberg SA, Trojanowski JQ, Traynor BJ, Smith BN, Topp S, Gkazi AS, et al..** Mutations in prion-like domains in hnRNPA2B1 and hnRNPA1 cause multisystem proteinopathy and ALS. *Nature 495, 467–473 (2013).*

66. **E., Carson JH and Barbarese.** Systems analysis of RNA trafficking in neural cells. . *Biol. Cell 97, 51–62 (2005).*
67. **Quaresma AJC, Oyama S, Barbosa JARG and Kobarg J.** The acidic domain of hnRNPQ (NSAP1) has structural similarity to Barstar and binds to Apobec1. . *Biochem. Biophys. Res. Commun. 350, 288–297 (2006).*
68. **Mizutani A, Fukuda M, Ibata K, Shiraishi Y and Mikoshiba K.** SYNCRIP, a cytoplasmic counterpart of heterogeneous nuclear ribonucleoprotein R, interacts with ubiquitous synaptotagmin isoforms. . *J. Biol. Chem. 275, 9823–9831 (2000).*
69. **Hobor F, Dallmann A, Ball NJ, Cicchini C, Battistelli C, Ogrodowicz RW, Christodoulou E, Martin SR, Castello A, Tripodi M, Taylor IA and Ramos A.** A cryptic RNA-binding domain mediates Syncrip recognition and exosomal partitioning of miRNA targets. *Nat Comm (2018) 9:831 DOI: 10.1038/s41467-018-03182-3.*
70. **Kabat JL, Barberan-Soler S and Zahler AM.** HRP-2, the Caenorhabditis elegans homolog of mammalian heterogeneous nuclear ribonucleoproteins Q and R, is an alternative splicing factor that binds to UCUAUC splicing regulatory elements. . *J. Biol. Chem. 284, 28490–28497 (2009).*
71. **Svitkin YV, Yanagiya A, Karetnikov AE, Alain T, Fabian MR, Khoutorsky A, Perreault S, Topisirovic I and Sonenberg N.** Control of translation and miRNA-dependent repression by a novel poly(A) binding protein, hnRNP-Q. *PLoS Biol. 11, e1001564 (2013).*
72. **McDermott SM, Meignin C, Rappsilber J and Davis I.** Drosophila Syncrip binds the gurken mRNA localisation signal and regulates localised transcripts during axis specification. *Biol. Open 1, 488–497 (2012).*
73. **McDermott SM, Yang L, Halstead JM, Hamilton RS, Meignin C and Davis I.** Drosophila Syncrip modulates the expression of mRNAs encoding key synaptic proteins required for morphology at the neuromuscular junction. *RNA 20, 1593–1606 (2014).*

74. **Williams KR, McAninch DS, Stefanovic S, Xing L, Allen M, Li W, Feng Y, Mihailescu MR and Bassell GJ.** hnRNP-Q1 represses nascent axon growth in cortical neurons by inhibiting Gap-43 mRNA translation. *Mol. Biol. Cell 27, 518–534 (2016).*
75. **Mourelatos Z, Abel L, Yong J, Kataoka N and Dreyfuss G.** SMN interacts with a novel family of hnRNP and spliceosomal proteins. . *EMBO J. 20, 5443–5452 (2001).*
76. **Chen HH, Chang JG, Lu RM, Peng TY and Tarn WY.** The RNA binding protein hnRNP Q modulates the utilization of exon 7 in the survival motor neuron 2 (SMN2) gene. . *Mol. Cell. Biol. 28, 6929–6938 (2008).*
77. **Yoo BC, Hong SH, Ku JL, Kim YH, Shin YK, Jang SG, Kim IJ, Jeong SY and Park JG.** Galectin-3 stabilizes heterogeneous nuclear ribonucleoprotein Q to maintain proliferation of human colon cancer cells. *Cell. Mol. Life. Sci. 66, 350–364 (2009).*
78. **Fenn S, Du Z, Lee JK, Tjhen R, Stroud RM and James TL.** Crystal structure of the third KH domain of human poly(C)-binding protein-2 in complex with a C-rich strand of human telomeric DNA at 1.6 A resolution. *Nucleic Acids Res. 2007;35(8):2651-60. Epub 2007 Apr 10.*
79. **Choi HS, Hwang CK, Song KY, Law PY, Wei LN and Loh HH.** Poly(C)-binding proteins as transcriptional regulators of gene expression. *Biochem Biophys Res Commun. 2009 Mar 13;380(3):431-6. doi: 10.1016/j.bbrc.2009.01.136. Epub 2009 Jan 27.*
80. **SA., Chkheidze AN and Liebhaber.** A novel set of nuclear localization signals determine distributions of the alphaCP RNA-binding proteins. *Mol Cell Biol. 2003 Dec;23(23):8405-15.*
81. **Choi HS, Song KY, Hwang CK, Kim CS, Law PY, Wei LN and Loh HH.** A proteomic approach for identification of a single-strand DNA-binding proteins involved in transcriptional regulationof mouse mu-opioid receptor gene. *Mol. Cell. Proteomics 7 (2008) 1517-1729.*

82. **Murray KE, Roberts AW and Barton DJ.** Poly(rC) binding proteins mediate poliovirus mRNA stability. *RNA (2001) 7:1126–1141.*
83. **R., Gamarnik AV and Andino.** Switch from translation to RNA replication in a positive-stranded RNA virus. *Genes & Dev (1998) 12: 2293–2304.*
84. **Blyn LB, Swiderek KM, Richards O, Stahl DC, Semler BL and Ehrenfeld E.** Poly(rC) binding protein 2 binds to stem-loop IV of the poliovirus RNA 59 noncoding region: Identification by automated liquid chromatography-tandem mass spectrometry . *Proc Natl Acad Sci USA 93:11115–11120+.*
85. **R., Gamarnik AV and Andino.** Two functional complexes formed by KH domain containing proteins with the 59 noncoding region of poliovirus RNA. . *RNA (1997) 3:882–892.*
86. **Shi H, Bencze KZ, Stemmler TL and Philpott CC.** A cytosolic iron chaperone that delivers iron to ferritin. *Science. 2008; 320:1207-1210.*
87. **Li Y, Lin L,Li Z, Ye X, Xiong K, Aryal B, Xu Z,Paroo Z, Liu Q, He C Jin P.** Iron Homeostasis Regulates the Activity of the MicroRNA Pathway through Poly(C)-Binding Protein 2. *Cell. Metab. 20122 Nov 2; 14(5):647-57.DOI 10.1016/j.cmet.2012.04.021.*
88. **Conigliaro, A., Amicone, L., Costa, V., De Santis Puzzonia, M., Mancone, C.,Sacchetti, B., Cicchini, C., Garibaldi, F., Brenner, D.A., Kisseleva, T., et al.** Evidence for a common progenitor of epithelial and mesenchymal components of the liver. *(2013).*
89. **Théry C, Witwer KW, Aikawa E, Alcaraz MJ, Anderson JD, Andriantsitohaina R, Antoniou A, Arab T, Archer F, Atkin-Smith GK, Ayre DC, Bach JM, Bachurski D, Baharvand H, Balaj L, Baldacchino S, Bauer NN et al..** Minimal information for studies of extracellular vesicles 2018 (MISEV2018): a position statement of the International Society for Extracellular Vesicles and update of the MISEV2014 guidelines. *J Extracell Vesicles. 2018 Nov 23;7(1):1535750. doi: 10.1080/20013078.2018.1535750. eCollection 2018.*

90. **Hill AF, Pegtel DM, Lambertz U, Leonardi T, O'Driscoll, L, Pluchino S, Ter-Ovanesyan D, and Nolte-'t Hoen EN.** ISEV position paper: extracellular vesicle RNA analysis and bioinformatics. *J. Extracell. Vesicles 2, 2.2013.*
91. **Heo I, Joo C, Kim YK, Ha M, Yoon MJ, Cho J, Yeom KH, Han J and Kim VN.** TUT4 in concert with Lin28 suppresses microRNA biogenesis through pre-microRNA uridylation. . *Cell 138, 696–708. 2009.*
92. **McHugh CA, Chen CK, Chow A, Surka CF, Tran C, McDonel P, Pandya- Jones A, Blanco M, Burghard C, Moradian A, et al.** The Xist lncRNA interacts directly with SHARP to silence transcription through HDAC3. *Nature 521, 232–236. 2015.*
93. **Battistelli C, Cicchini C, Santangelo L, Tramontano A, Grassi L, Gonzalez FJ, de Nonno V, Grassi G, Amicone L and Tripodi M.** The Snail repressor recruits EZH2 to specific genomic sites through the enrollment of the lncRNA HOTAIR in epithelial-to-mesenchymal transition. *Oncogene, Published online July 25, 2016. http://dx.doi.org/10.1038/onc.2016.26.*
94. **Pasque V, Gillich A, Garrett N and Gurdon JB.** Histone variant macroH2A confers resistance to nuclear reprogramming. . *EMBO J. 30, 2373–2387. (2011).*
95. **Ao W, Gaudet J, Kent WJ, Muttumu S and Mango SE.** Environmentally induced foregut remodeling by PHA-4/FoxA and DAF-12/NHR. . *Science 305, 1743–1746.(2004).*
96. **Eiring AM, Harb JG, Neviani P, Garton C, Oaks JJ, Spizzo R, Liu S, Schwind S, Santhanam R, Hickey CJ, Becker H, Chandler JC, Andino R, Cortes J, Hokland P, Huettner CS, Bhatia R, Roy DC, Liebhaber SA, Caligiuri MA, Marcucci G, Garzon R et al.,.** miR-328 Functions as an RNA Decoy to Modulate hnRNP E2 Regulation of mRNA Translation in Leukemic Blasts. *Cell. 2010 Mar 5;140(5):652-65. doi: 10.1016/j.cell.2010.01.007.*